EBioMedicine xxx (2019) xxx

Contents lists available at ScienceDirect

EBioMedicine

journal homepage: www.ebiomedicine.com

EBioMedicine
Published by THE LANCET

Tobacco smoking induces changes in true DNA methylation, hydroxymethylation and gene expression in bronchoalveolar lavage cells

Mikael V. Ringh [a,*], Michael Hagemann-Jensen [b], Maria Needhamsen [a], Lara Kular [a], Charles E. Breeze [c,d], Louise K. Sjöholm [a], Lara Slavec [a], Susanna Kullberg [b,e], Jan Wahlström [b], Johan Grunewald [b], Boel Brynedal [f], Yun Liu [g], Malin Almgren [a], Maja Jagodic [a], Johan Öckinger [b], Tomas J. Ekström [a,*]

[a] Department of Clinical Neuroscience, Karolinska Institutet, Center for Molecular Medicine, Stockholm, Sweden
[b] Department of Medicine, Karolinska Institutet, Center for Molecular Medicine, Stockholm, Sweden
[c] Altius Institute for Biomedical Sciences, Seattle, USA
[d] UCL Cancer Institute, University College London, London, United Kingdom
[e] Department of Respiratory Medicine, Theme Inflammation and Infection, Karolinska University Hospital, Stockholm, Sweden
[f] Institute of Environmental Medicine, Karolinska Institutet, Stockholm, Sweden
[g] Department of Biochemistry and Molecular Biology, School of Basic Medical Sciences, Fudan University, Shanghai, China

ARTICLE INFO

Article history:
Received 9 May 2019
Received in revised form 28 June 2019
Accepted 2 July 2019
Available online xxxx

Keywords:
DNA methylation
DNA hydroxymethylation
Enhancers
EPIC
Epigenetics
Smoking
Oxidative stress
Alveolar macrophages

ABSTRACT

Background: While smoking is known to associate with development of multiple diseases, the underlying mechanisms are still poorly understood. Tobacco smoking can modify the chemical integrity of DNA leading to changes in transcriptional activity, partly through an altered epigenetic state. We aimed to investigate the impact of smoking on lung cells collected from bronchoalveolar lavage (BAL).

Methods: We profiled changes in DNA methylation (5mC) and its oxidised form hydroxymethylation (5hmC) using conventional bisulphite (BS) treatment and oxidative bisulphite treatment with Illumina Infinium MethylationEPIC BeadChip, and examined gene expression by RNA-seq in healthy smokers.

Findings: We identified 1667 total 5mC + 5hmC, 1756 5mC and 67 5hmC differentially methylated positions (DMPs) between smokers and non-smokers (FDR-adjusted $P < .05$, absolute $\Delta\beta > 0.15$). Both 5mC DMPs and to a lesser extent 5mC + 5hmC were predominantly hypomethylated. In contrast, almost all 5hmC DMPs were hypermethylated, supporting the hypothesis that smoking-associated oxidative stress can lead to DNA demethylation, via the established sequential oxidation of which 5hmC is the first step. While we confirmed differential methylation of previously reported smoking-associated 5mC + 5hmC CpGs using former generations of BeadChips in alveolar macrophages, the large majority of identified DMPs, 5mC + 5hmC (1639/1667), 5mC (1738/1756), and 5hmC (67/67), have not been previously reported. Most of these novel smoking-associating sites are specific to the EPIC BeadChip and, interestingly, many of them are associated to FANTOM5 enhancers. Transcriptional changes affecting 633 transcripts were consistent with DNA methylation profiles and converged to alteration of genes involved in migration, signalling and inflammatory response of immune cells.

Interpretation: Collectively, these findings suggest that tobacco smoke exposure epigenetically modifies BAL cells, possibly involving a continuous active demethylation and subsequent increased activity of inflammatory processes in the lungs.

Fund: The study was supported by the Swedish Research Council, the Swedish Heart-Lung Foundation, the Stockholm County Council (ALF), the King Gustav's and Queen Victoria's Freemasons' Foundation, Knut and Alice Wallenberg Foundation, Neuro Sweden, and the Swedish MS foundation.

1. Introduction

Although tobacco smoking is a well-known toxic agent with serious impact on human health, smoking or exposure to smoke remains common worldwide. Smoke exposure is a risk factor and a common cause of death from cardiovascular disease, chronic obstructive pulmonary disease (COPD) and multiple types of cancer, in particular lung cancer

Abbreviations: BAL, Bronchoalveolar lavage; BS, Bisulphite; DMP, Differentially methylated position; DMR, Differentially methylated region; DVP, Differentially variable position; IPA, Ingenuity Pathway Analysis; oxBS, Oxidative bisulphite; RNA-seq, RNA sequencing; TF, Transcription factor; 5hmC, 5-hydroxymethylcytosine; 5mC, 5-methylcytosine.

* Corresponding authors.
E-mail addresses: mikael.ringh@ki.se (M.V. Ringh), tomas.ekstrom@ki.se (T.J. Ekström)

https://doi.org/10.1016/j.ebiom.2019.07.006

Research in Context

Evidence before this study

Tobacco smoking can lead to epigenetic and transcriptional changes in several tissues, and is a well-known risk factor for development of a multiple diseases. There is a growing list of smoking-associated epigenetic biomarkers in blood cells, as well as novel sites in other affected tissues. We searched for articles in PubMed using various combinations of the search terms "DNA methylation", "DNA hydroxymethylation", "EPIC", "850 K", "Smoking", and "Alveolar macrophages" (last search April 30th 2019). Two studies on DNA methylation in alveolar macrophages from smokers were identified, one investigating ~25,000 CpG loci (n = 22), and the other ~450,000 (n = 19). These studies have presented evidence of genome-wide changes in total DNA methylation and transcription in alveolar macrophages (lung macrophages), using previously available techniques.

Added value of this study

The present study provides new fundamental information on smoking-associated effects on DNA methylation and transcription in alveolar macrophage-dense BAL cells. Oxidative stress is induced by tobacco smoking, and also links to a DNA demethylation pathway where 5-methylcytosine (5mC), as a first step, is oxidised to 5-hydroxymethylcytosine (5hmC). We investigated smoking-associated DNA methylation and hydroxymethylation changes in bronchoalveolar lavage (BAL) cells, and to the best of our knowledge, this is the first epigenome-wide study identifying differentially hydroxymethylated CpG sites as well as true 5mC sites associated with smoking (n = 35) in any human tissue. It is also the first study on lung cells using the recently released Illumina EPIC BeadChip, covering >850,000 CpG loci. Predominant 5mC hypomethylation in contrast to predominant 5hmC hypermethylation supports the hypothesis of a DNA demethylation process initiated by smoking-induced oxidative stress. Notably, many of the affected loci were located at enhancers. We also investigated transcriptional changes using RNA-seq, and found converging alterations in the transcriptome and methylome, with genes involved in signalling, migration, and inflammatory response of immune cells.

Implications of all the available evidence

The current study provides new insights into understanding the impact of tobacco smoking on human health. We could confirm many differentially methylated sites from previous analyses of alveolar macrophages as well as blood cells. Importantly, we also demonstrate novel findings including differential methylation/hydroxymethylation at specific loci together with transcriptional effects, and find previously unreported pathways. These findings provide information that may be of relevance in inflammatory processes leading up to disease. Further studies are warranted to explore the DNA demethylation pathway in the context of smoking-induced oxidative stress.

[1]. Tobacco smoking is also a risk factor for autoimmune diseases, most notably rheumatoid arthritis (RA) and multiple sclerosis (MS) for which there is an established gene-environment interaction with specific HLA risk alleles, resulting in a substantially elevated risk for developing diseases [2,3]. Cigarette smoke contains a complex mixture of >6000 chemicals, many of them reaching the lower airways during smoke inhalation [4]. Deep airway alveolar macrophages, which in healthy individuals constitute the majority of bronchoalveolar lavage (BAL) cells, play pivotal roles in clearance of such inhaled particles and debris and initiation of inflammatory response [5]. Overall, both the local pro-inflammatory and oxidative response caused by cigarette smoke inhalation, as well as the systemic impact of smoke exposure can lead to long-term deleterious effects on health [6]. Epigenetic mechanisms have been proposed to mediate some of the impact of cigarette smoke through changes in DNA methylation, which may alter gene expression and contribute to smoking-associated disease [7]. With the development of DNA methylation arrays, the effect of smoking on total DNA methylation has been extensively studied in blood cells from adults, showing marked differences in smokers compared to non-smokers [7–9], which can be even more pronounced in patients, as shown in MS smokers [10]. The effect of tobacco smoking on DNA methylation is also evident in cells from cord blood [11] and blood [12] from newborns, whose mothers smoked during pregnancy. However, only a few studies have investigated DNA methylation in bronchoalveolar immune cells [13,14], which regulate inflammatory reactions through secretion of modulatory and proinflammatory signal molecules, and are affected directly by tobacco smoke.

DNA methylation plays an important role as transcriptional regulator in many biological contexts, such as cell differentiation, embryogenesis, genomic imprinting, and development of disease [15]. In mammals, DNA methylation is most commonly found as 5-methylcytosine (5mC) in the context of CpG dinucleotides and has been associated with gene regulation, where gene promoter methylation usually exerts a repressive action on transcription [16]. In addition to traditional 5mC, other forms of cytosine DNA modifications have been identified, deriving from a DNA demethylation pathway with sequential oxidation of 5mC by the TET family of enzymes, to 5-hydroxymethylcytosine (5hmC) [17], 5-formylcytosine (5fC), and 5 carboxylcytosine (5caC) [18,19]. Hydroxymethylated cytosine (5hmC), often referred to as the sixth base, is however not only an intermediary step of active demethylation, but also a stable epigenetic mark with unique functional properties such as binding of transcription factors and positive regulation of gene expression [20,21].

Recent studies have demonstrated that the DNA demethylation pathway can be initiated by oxidative stress [22,23]. Briefly, oxidative DNA damage from reactive oxygen species (ROS) leads to formation of 8-oxoguanine (8-oxoG), an oxidised product of guanine, and subsequent oxidation of adjacent 5mC to 5hmC [22]. However, conventional bisulphite (BS) conversion used to detect DNA methylation is not able to distinguish 5mC from 5hmC [24]. Therefore, most of the previously published DNA methylation data are reporting overall signal from a mixture of both modifications. In that context, DNA methylation studies in BAL cells (primarily alveolar macrophages) have identified smoking-associated differentially methylated positions (DMPs) using Infinium HumanMethylation27 BeadChip [13] and Infinium HumanMethylation450 BeadChip [14]. In this study, we hypothesised that oxidative stress caused by smoking [25], might affect not only 5mC but also 5hmC patterns in the lung as part of DNA demethylation. In order to better comprehend the effect of tobacco smoking on pulmonary cells, we examined DNA methylation and hydroxymethylation in healthy smokers and non-smokers using the latest Illumina HumanMethylation EPIC BeadChip, covering over 850 K CpG sites and thus providing a higher coverage compared to previous arrays. Further, we combined DNA methylation analysis with gene expression analysis using RNA-seq in BAL cells from healthy smokers and non-smokers.

2. Material and methods

2.1. Study subjects, bronchoscopy and bronchoalveolar lavage

We obtained 49 BAL samples from healthy volunteers (20 smokers, 29 non-smokers) collected during bronchoscopy as

Please cite this article as: M.V. Ringh, M. Hagemann-Jensen, M. Needhamsen, et al., Tobacco smoking induces changes in true DNA methylation, hydroxymethylation and gene expression in b..., EBioMedicine, https://doi.org/10.1016/j.ebiom.2019.07.006

previously described [26]. All subjects gave their written consent, and the study was approved by the Regional Ethical Review Board in Stockholm. None of the subjects had clinically relevant airway infections or allergy symptoms at the time of bronchoscopy, and subjects diagnosed with asthma, COPD, other lung diseases, or other inflammatory conditions were not included in the study. All subjects filled out questionnaires regarding general and pulmonary health, current medications, and previous and current smoking habits, and in addition also underwent dynamic spirometry (Medikro PRO, Aiolos Medical). Individuals with >5 pack years (pack years = (cigarettes smoked per day / 20) x years smoking), or smoking at least 5 cigarettes per day, were defined as smokers. Non-smokers were defined as individuals who has never smoked. All subjects have been included in a previous study [27].

2.2. Differential cell count, DNA and RNA extraction

BAL cells and fluid were separated by centrifugation (400 ×*g* at 4 °C for 10 min), and the supernatants were immediately stored at -80 °C for later use. Approximately 500.000 BAL cells were collected and resuspended in RPMI 1640 without supplements. Smears for differential cell counts were prepared by cytocentrifugation (Cytospin 2, Shanon Ltd) at 22 g for 3 min and stained with May-Grünwald Giemsa, or toluidine/hematoxylin for mast cell identification. A minimum of 500 cells/sample was counted, to estimate cellular proportions in BAL. Samples with low alveolar macrophage content (< 80%) were not included in the study. Genomic DNA and total RNA were extracted using the AllPrep DNA/RNA/miRNA Universal Kit (Qiagen) according to the manufacturer's protocol. The concentration of both DNA and total RNA were quantified using PicoGreen (Invitrogen) and Qubit 3 fluorometer (Invitrogen).

2.3. Total 5mC + 5hmC and 5mC methyl processing

DNA from BAL cells was processed using the TrueMethyl conversion kit (Cambridge Epigenetix) workflow in order to investigate true methylation (5mC) by using oxidative bisulphite treatment (oxBS), and total methylation (5mC + 5hmC) by regular common non-oxidative bisulphite treatment (BS). DNA methylome profiling was carried out using the Infinium HumanMethylationEPIC BeadChip Kit (Illumina), which interrogates over 850,000 CpG sites. Methylation arrays were processed by the National Genomics Infrastructure (NGI), Science for Life Laboratory at Uppsala University. Samples were randomised according to smoking-status, age, gender, and cell-proportion and processed together with technical replicates in one run. DNA methylation β-values from the technical replicates correlated strongly with a Pearson correlation value of 0.992 ($P = 2.2 \times 10^{-16}$). Raw intensity IDAT format files were used for subsequent array analysis.

2.4. Generation of RNA sequencing libraries

RNA integrity number (RIN) measurements were performed on an Agilent Bioanalyzer using the RNA 6000 nano kit (Agilent Technologies). 150 ng of total RNA from each individual was used to generate poly-A selected SMART-seq2 cDNA libraries according to the published protocol [28], with minor adjustments to fit bulk RNA input. Spike-in ERCC (External RNA Controls Consortium) RNA was added at 10.000× dilution and cDNA received 6 rounds of preamplification. Sequence ready libraries was prepared with Illumina Nextera index primers using in-house produced TN5 tagmentation enzyme according to following protocol [29]. All libraries were pool and purified with Ampure XP beads, and sequenced at 125 bp paired-end on an Illumina HiSeq 2500.

2.5. Normalisation of 5mC + 5hmC and 5mC methyl data

Raw IDAT files were imported and processed in R software (version 3.5.2) using minfi (version 1.28.4) [30,31] and ChAMP (version 2.12.4) [32] packages. BS and oxBS samples from the same individual were run on the same array. We compared two different normalisation strategies, stratified quantile normalisation (SQN) and subset-quantile within array normalisation (SWAN) [33] and obtained similar results. Final normalisation was done with SQN, and BS-treated (5mC + 5hmC) and oxBS-treated (5mC) samples were processed separately.

Methylation signals were computed as β-values, ranging from 0 to 1. β-values from BS-treated samples represent the total methylation, including both 5hmC and 5mC. The β-values from oxBS-treated samples represent true methylation, and only include 5mC. Samples with probe coverage <95% were removed, as well as probes with a detection *P* value >.01 in >5% of samples. Further, sex chromosome, cross-reactive and SNP-related probes were removed [34], resulting in 43 samples with 764,958 total 5mC + 5hmC probes and 36 samples with 736,336 true 5mC probes. Finally, only probes and samples overlapping between the datasets were kept, resulting in 35 samples with both 5mC and 5mC + 5hmC readings of 735,794 probes (Supplementary Fig. 1).

2.6. Genomic annotation of CpG sites

Genomic regions were annotated using HumanMethylationEPIC probe annotations through the ChAMP [32] Bioconductor package. The following categories were used as locations in relation to gene: TSS1500 (200 to 1500 nucleotides, nt, upstream of transcription start site, TSS); TSS200 (up to 200 nt upstream of TSS); 5′ UTR (5′ untranslated region); 1st exon; Body (gene body); ExonBnd (exon boundaries), IGR (intergenic regions), and 3′ UTR (3′ untranslated region). Annotations related to CpG islands (CGIs) were divided into following categories: CGIs, CGI shores (flanking shore regions, <2 kb up- and downstream of CGIs), CGI shelfs (2–4 kb up- and downstream of CGIs), and open sea (non-CGI-related sites). Venn diagrams were created using the R package VennDiagram (version 1.6.20) [35].

2.7. Differential methylation and variability analysis

DMP analysis of 5mC + 5hmC and 5mC were done on M-values after transformation from β-values ($M = \log2(\beta/(1-\beta))$ as previously recommended [36]. We used a linear model (limma) with the empirical Bayes approach with non-smokers as the reference group and adjusted for covariates (age and sex). A probe was considered significantly differentially methylated if the methylation difference (β-values) between the smokers and non-smokers were at least 15% with a FDR-adjusted (Benjamini-Hochberg) *P* value <.05. For hydroxymethyl (5hmC) DMP finding, normalised 5mC (oxBS) β-values were subtracted from normalised 5mC + 5hmC β-values to calculate the hydroxymethyl level (Δβ) at each probe. Similarly to previous analysis we used limma with empirical Bayes approach adjusting for age and sex. Additionally, since oxBS treatment is known to introduce negative β-values when subtracting 5mC from 5mC + 5hmC, we performed a second limma where negative β-values were set to a value close to zero (1×10^{-7}). We combined the two methods and only 5hmC DMPs that overlapped between the generated lists were considered significant to limit false positives. The RUVm method [37] was used to generate a comparison dataset where unwanted variation was removed. Instead of using known covariates, which can be limited by inaccurate measurements, this method only assume the presence of hidden covariates. A linear regression model with ebayes was run on smoking status yielding statistically non-significant CpGs (FDR-adjusted *P* value >.5) that were treated as negative control probes, i.e. not associated with smoking. Next, RUVfit was run using RUV-inverse function, and then adjusted through RUVadj (FDR-adjusted *P* value <.05).

Please cite this article as: M.V. Ringh, M. Hagemann-Jensen, M. Needhamsen, et al., Tobacco smoking induces changes in true DNA methylation, hydroxymethylation and gene expression in b..., EBioMedicine, https://doi.org/10.1016/j.ebiom.2019.07.006

In addition to the single site DMP analysis, we applied the DMRcate package (version 1.18.0) [38] with default settings to detect differentially methylated regions (DMRs) between smokers and non-smokers. We fitted a linear model of methylation values at each probe as a function of smoking status and adjusting for covariates (age, sex). DMRs were defined as those with Stouffer-transformed limma-derived FDR-adjusted *P* values <.05. Identified DMRs were also filtered using cut-off values of mean absolute Δβ >15%.

Analysis of differential variability was applied to identify smoking-associated DVPs (differential variability positions). DiffVar first uses an empirical Bayes Levene-type algorithm to calculate absolute deviations from respective group means, then uses moderated *t*-test to compare the distribution of deviations between the groups, assuming that the variability is driven by a range of outliers and not just a few. Age and sex were included as covariates, and DVPs were defined as sites with and FDR-adjusted *P* value <.05.

A significant DMP associated with the gene body of *ITSN1* (cg11650372) was selected based on significance and Δβ and was validated both with oxidative and non-oxidative BS pyrosequencing. Primers were designed using the PyroMark Assay Design 2.0 software and afterwards optimised for best annealing temperature (Supplementary Table 1). 1 μL of oxidised and non-oxidised converted DNA (10 ng) was used for PCR amplification with the PyroMark PCR kit (Qiagen). The product was used together with streptavidin Sepharose high-

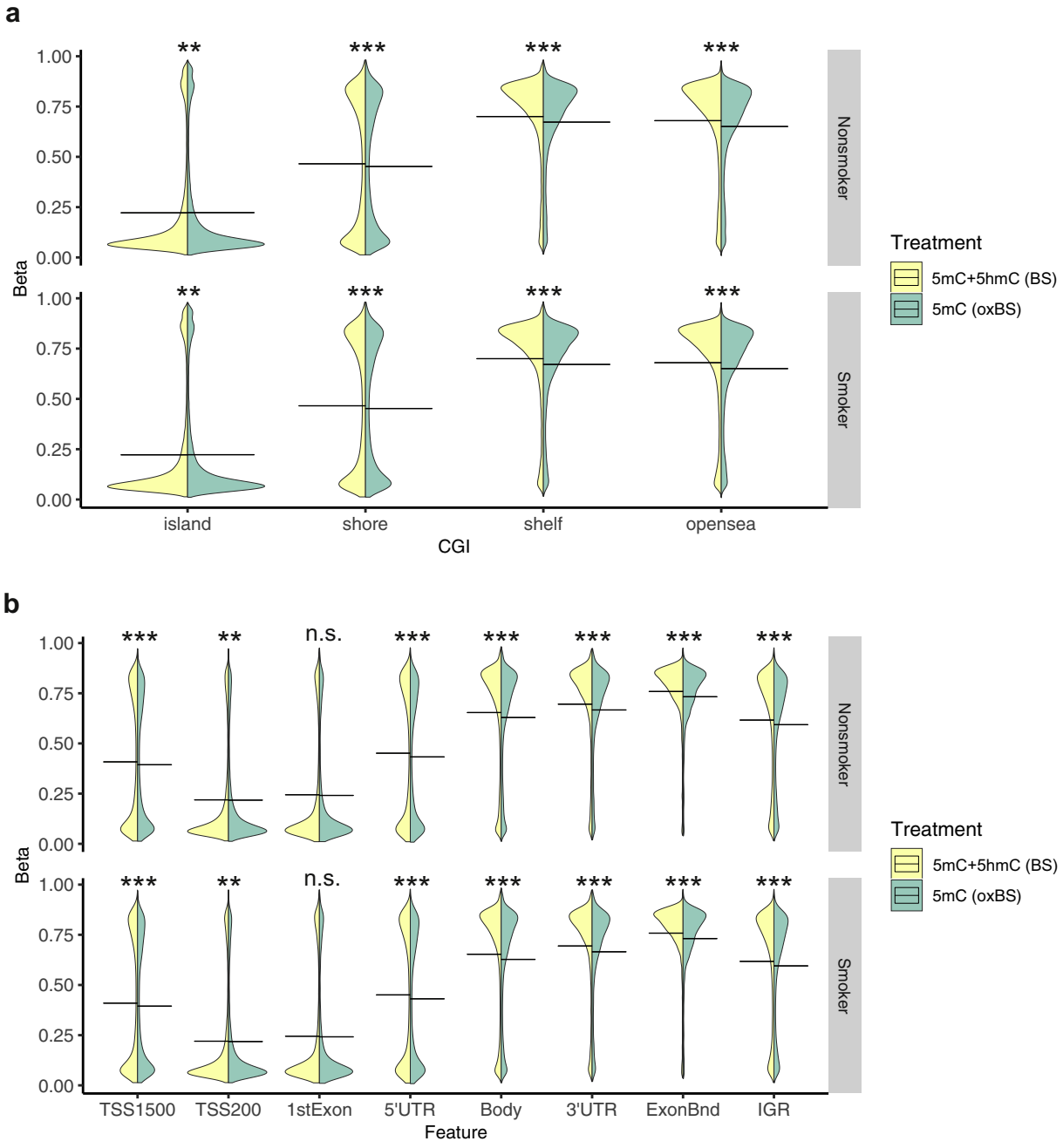

Fig. 1. Feature-specific differences in β-value distribution between total 5mC + 5hmC and true 5mC. Violin plots representing the distribution of β-values from 735,794 probes after SQN normalisation, plotted as densities in relation to CpG islands (**a**) and genomic features (**b**). Yellow plots represent standard bisulphite-treated samples with a combination of both 5mC and 5hmC (total BS methyl). Green plots represent oxidative bisulphite-treated samples with 5mC (true 5mC, oxBS). Plots representing smoker densities are shown in upper rows (**a-b**) and non-smoker plots in lower rows (**a-b**). Differences in distributions between 5mC and 5mC + 5hmC was tested using Wilcoxon signed-rank test was considered significant with a *P* value <.05. * $P < .05$; ** $P < .01$; *** $P < .001$; n.s = not significant. (For interpretation of the references to colour in this figure legend, the reader is referred to the web version of this article.)

Please cite this article as: M.V. Ringh, M. Hagemann-Jensen, M. Needhamsen, et al., Tobacco smoking induces changes in true DNA methylation, hydroxymethylation and gene expression in b..., EBioMedicine, https://doi.org/10.1016/j.ebiom.2019.07.006

performance beads (GE Healthcare), the respective sequencing primer, and PyroMark Gold Q96 reagent kit (Qiagen), for pyrosequencing with the PSQ 96 system (Qiagen). Data were analysed on the PyroMark Q96 software.

2.8. Identification of cell-type specific signal and transcription factor analysis with eFORGE analyses

In order to account for differences in cell-type composition in BAL, and identify if they might influence the observed methylation differences, we performed analyses with eFORGE (experimentally derived Functional element Overlap analysis of ReGions from EWAS) [39]. As input, eFORGE accepts a minimum of 20 and a maximum of 1000 CpG sites, in our case including the top 1000 DMPs for total methyl and 5mC, and 67 CpG sites for 5hmC. We examined enrichments for DNase I hypersensitive sites (DHSs) and histone marks (H3K27me3, H3K36me3, H3K4me3, H3K9me3, and H3K4me1). Default settings were used when running the analysis. An in-house pipeline for eFORGE-TF analysis was used to investigate TF motif associations. TF motifs were linked back to a TF gene list and analysed with PANTHER pathway analysis.

2.9. Differential expression analysis

RNA sequencing reads were quality filtered and trimmed for adapters using TrimGalore (version 0.6.0) at default parameters. Afterwards the filtered reads were processed using the pseudoalignment-based Kallisto algorithm (version 0.45.0) with GENCODE v24 comprehensive transcript set as reference transcriptome. For downstream analysis, only samples with a RIN value above 7 were included, and only genes with >10 normalised read counts were kept. In total 23 samples passed these criteria, 10 smokers and 13 non-smokers, which were used for differential expression analysis using DESeq2 package in R. We adjusted for the covariates sex and age and only considered genes with a BH-adjusted (FDR) P value <.05 as significant, together with an absolute log2 fold change threshold >1.

2.10. Gene ontology analyses

Gene ontology (GO) analysis was performed using Ingenuity Pathway Analysis (IPA) (Qiagen) on the annotated genes from 5mC + 5hmC and 5mC DMP genes (FDR-adjusted $P < .05$, absolute $\Delta\beta > 0.15$; 928 and 938 genes, respectively), differentially expressed genes (adj. P value <.05, logFC >1, 633 genes) as well as dysregulated genes that harbour 5mC + 5hmC DMPs (70 genes), applying unbiased parameters for all criteria including tissues selection. GO analysis was also performed on annotated genes from 5hmC DMP genes (nominal $P < .001$, absolute $\Delta\beta > 0.05$; 983 genes). Right-tailed Fisher's exact test was used to calculate P values, with $P < .05$ considered statistically significant. We confirmed IPA findings using over-representation analysis (www.webgestalt.org) [40] on differentially expressed genes and annotated 5mC + 5hmC DMPs genes. Comparison between findings from gene expression and DNA methylation analyses was performed using REVIGO tool [41] based on multidimensional scaling of overrepresented GO terms with semantic similarities. STRING network was generated using STRING database version 10.5 with a minimum level of confidence >0.4.

2.11. Statistical analysis

Statistical methods used for genome-wide DNA methylation and gene expression analyses are detailed in the previous sections. For feature-specific distribution analysis of β-values, we used Wilcoxon rank sum test with Bonferroni adjusted P values for multiple comparison. For enrichment and depletion analysis of differential methylation, we used Pearson's Chi-squared test on contingency tables of count data, and adjusted for multiple comparison using Bonferroni. Correlation analysis between β-values and normalised gene counts was performed using Pearson method, and the Spearman method for correlation analysis between β-values and macrophage fractions. Power analysis (post-hoc) was performed using the pwrEWAS package [42], a tool designed specifically for power analysis of EWAS studies. Input parameters were as follows; 735.000 CpGs, 1700 target CpGs, minimum $\Delta\beta$ detection limit 0.05, FDR-adjusted P value <.05, and adult PBMC as the closest available tissue.

2.12. Data availability

DNA methylation data from this study is available in Gene Expression Omnibus (GEO) database under accession number GSE133062, and RNA-seq data is available upon request.

3. Results

3.1. Characteristics of study participants

Our study included a total of 49 healthy volunteers who all underwent bronchoscopy with bronchoalveolar lavage (BAL), spirometry, and clinical assessment. Quality checks and filtering described in Supplementary Fig. 1 resulted in 35 DNA methylation samples (14 smokers and 21 non-smokers) and 23 RNA-seq samples (10 smokers and 13 non-smokers) for further analyses. Description of the cohort and cell counts is shown in Table 1. Smokers and non-smokers were similar in age (median 28 vs 24 years, P = ns) and both included a larger proportion of females with non-significant difference between groups (P = ns). Smokers displayed a significant increase in BAL fluid cell concentration ($P < .001$), as well as an altered cellular composition compared to non-smokers (Table 1). More specifically, alveolar macrophages proportion was higher ($P < .001$) and lymphocytes proportion lower ($P < .001$) in smokers compared to non-smokers while

Table 1
Characterisation of healthy individuals included in our study.

	All subjects	Non-smokers	Smokers
Subject	35	21	14
Sex (male/female)	13/22	9/12	4/10
Age (years)	25.0 [22.0–29.0]	24.0 [22.0–28.0]	28.0 [24.3–29.8]
Cigarettes/day	12.5 [10.0–19.8]	N/A	12.5 [10.0–19.8]
Pack years	6.0 [5.0–9.5]	N/A	6.0 [5.0–9.5]
FEV1, % predicted	103.0 [97.5–110.5]	103.0 [98.0–107.0]	105.0 [94.8–110.8]
FVC, % predicted	109.0 [102.0–117.0]	108.0 [102.0–117.0]	110.5 [103.0–115.3]
FEV/FVC %	81.0 [78.0–83.5]	82.0 [79.0–83.0]	80.0 [76.5–84.5]
BALF cell concentration ($x10^6$/L)	119.6 [75.4–254.9]	76.8 [72.2–105.4]	300.6 [219.0–357.5]***
BAL recovery (%)	71.0 [62.5–77.5]	74.0 [70.0–79.0]	64.0 [58.0–69.5]**
BAL macrophages (%)	93.4 [88.9–96.1]	90.8 [85.8–93.4]	96.5 [93.8–97.4] ***
BAL lymphocytes (%)	4.8 [2.8–9.7]	7.3 [4.2–12.0]	2.2 [1.8–3.45]***
BAL neutrophils (%)	0.8 [0.4–1.3]	1.0 [0.6–2.0]	0.7 [0.4–1.15]
BAL eosinophils (%)	0.2 [0–0.4]	0.2 [0–0.3]	0.1 [0–0.4]
BAL basophils (%)	0 [0–0]	0 [0–0]	0 [0–0]
BAL mast cells (%)	1.0 [0–2.5]	0 [0–3.0]	1.0 [0.3–2.0]
BAL CD4/CD8 ratio	1.6 [1.1–2.7]	1.9 [1.4–3.0]	1.1 [0.8–1.8]

Basic characterisation of individuals included in our cohort. Data represent n or median [25th–75th percentile]. Pack years: (cigarettes smoked per day / 20) x years smoking); FEV1: forced expiratory volume in 1 s; FVC: forced vital capacity; BALF: bronchoalveolar lavage fluid; BAL: bronchoalveolar lavage; N/A: not applicable. Statistics calculated using Chi-square test for male/female ratio and Mann-Whitney U test for other comparisons: * $P < .05$ compared to non-smokers, ** $P < .01$ compared to non-smokers, *** $P < .001$ compared to non-smokers.

Please cite this article as: M.V. Ringh, M. Hagemann-Jensen, M. Needhamsen, et al., Tobacco smoking induces changes in true DNA methylation, hydroxymethylation and gene expression in b..., EBioMedicine, https://doi.org/10.1016/j.ebiom.2019.07.006

other cellular compartments remained unchanged. Altogether, the composition of BAL fluid is consistent with previous analyses of smoking and non-smoking healthy volunteers [43].

3.2. Genomic profiling of total 5mC + 5hmC and 5mC reveals feature-specific presence of hydroxymethyl in BAL cells

We determined genome-wide total 5mC + 5hmC and 5mC CpG levels in BAL cells from smokers and non-smokers using the Illumina HumanMethylationEPIC BeadChip. The array covers over 850 K CpG sites with improved coverage of regulatory elements compared to its 27 K and 450 K predecessors, including 58% of Functional Annotation of the Mammalian Genome 5 (FANTOM5) enhancers. Total methylation (5mC + 5hmC) was quantified using BS-treated (bisulphite-treated) DNA samples and represents a combination of 5mC + 5hmC signals. In order to decipher the contribution of 5mC from 5hmC signals we performed oxidative BS (oxBS) treatment in parallel to BS treatment prior to array hybridisation. After QC and filtering steps (Supplementary Fig. 1), we retained 35 subjects for further analysis, with overlapping oxBS and BS data and 735,794 probes in common.

As an exploratory first step, we examined distributions of all 735,794 probes focusing on the genomic features related to CpG island (CGI) (Fig. 1a), and gene location (Fig. 1b). BAL cells from both smokers and non-smokers had a significantly higher 5mC + 5hmC than 5mC for probes located in open sea, shelfs and shore regions (Wilcoxon rank sum test, $P < .001$). The probe distribution was also significantly different between smokers and non-smokers in open sea ($P < .001$) and shelf regions (5mC + 5hmC $P < .01$, 5mC $P < .05$; Supplementary Fig. 2a). Since the subtraction of true 5mC values from 5mC + 5hmC values results in 5hmC values, our data suggest a genome-wide presence of 5hmC in BAL cells across CGI-related features, most likely outside CGI as the typically low CGI methylation levels is less permissive to demethylation. Similar to reports describing other peripheral tissues [44], we observed relatively low overall levels of 5hmC in BAL cells.

Exploration of DNA methylation signals throughout the genome revealed significant differences in distribution between 5mC + 5hmC and 5mC signals (Fig. 1b). No significant difference was observed between 5mC + 5hmC and 5mC signal in 1st exon, displaying low range of methylation distribution in both smokers and non-smokers. Overall, distribution profiles at promoter regions (defined here as TSS200 + TSS1500) indicated low methylation. Smokers and non-smokers displayed relatively similar 5mC + 5hmC and 5mC signal distribution across all genomic regions, but with significant differences in gene bodies and IGR ($P < .001$; Supplementary Fig. 2b). Thus, global differences between total 5mC + 5hmC and true 5mC (oxBS) methylation profiles indicate presence of 5hmC in BAL cells.

3.3. Site and feature-specific changes in total 5mC + 5hmC, 5mC, and 5hmC in BAL cells from smokers

To determine genome-wide differences in total 5mC + 5hmC and true DNA methylation (5mC) between smokers and non-smokers in BAL cells, we applied a linear regression model with age and sex included as covariates and with a Benjamini-Hochberg (FDR) adjusted level of significance of $P < .05$. We set a stringent delta beta ($\Delta\beta$) cut-off of 15% for differential methylation, which was substantially higher

Table 2
Summary of the top 10 significant smoking-associated DMPs of total 5mC + 5hmC (BS), true 5mC (oxBS), and 5hmC.

Probe	adj.P.Val	Chr	Position	Gene	Delta Beta	Island Relation	Feature	Enh	450 k chip	Blood	AMs 450 k	DMP overlap
5mC + 5hmC DMPs												
cg04857037	3.77E-12	1	26,136,971	*SEPN1*	−0.24	OpenSea	Body					5mC
cg04308301	4.68E-12	8	131,454,686	*ASAP1*	−0.21	N_Shore	5'UTR	*				5mC
cg26721868	8.01E-12	19	4,567,641		−0.38	S_Shore	IGR		*			5mC
cg02233197	9.41E-11	15	51,390,542	*TNFAIP8L3*	−0.30	S_Shelf	Body		*		*	5mC
cg04135110	1.72E-10	5	346,695	*AHRR*	0.19	S_Shelf	Body		*	*		5mC
cg01596674	2.01E-10	9	130,342,290	*FAM129B*	−0.22	OpenSea	TSS1500		*			5mC
cg12617080	2.95E-10	1	156,509,844	*IQGAP3*	−0.25	OpenSea	Body		*			5mC
cg01668352	3.27E-10	12	64,482,597	*SRGAP1*	−0.30	OpenSea	Body		*	*	*	5mC
cg21513724	3.27E-10	10	105,409,153	*SH3PXD2A*	−0.23	OpenSea	Body	*				5mC
cg14223856	5.35E-10	9	139,508,740		−0.32	OpenSea	IGR		*		*	5mC
5mC DMPs												
cg02233197	2.39E-09	15	51,390,542	*TNFAIP8L3*	−0.29	S_Shelf	Body		*		*	BS
cg26721868	2.39E-09	19	4,567,641		−0.26	S_Shore	IGR		*			BS
cg14223856	5.30E-09	9	139,508,740		−0.40	OpenSea	IGR		*		*	BS
cg10655682	3.49E-08	19	4,567,177		−0.34	S_Shore	IGR	*				BS
cg11180972	3.49E-08	12	105,066,468	*CHST11*	−0.29	OpenSea	Body	*				BS
cg25711726	3.49E-08	11	124,949,155	*SLC37A2*	−0.34	OpenSea	ExonBnd					BS
cg07457727	3.49E-08	8	131,451,983		−0.30	N_Shelf	IGR		*		*	BS
cg09552070	3.49E-08	17	3,704,607	*ITGAE*	−0.22	OpenSea	TSS200					BS
cg04135110	4.88E-08	5	346,695	*AHRR*	0.20	S_Shelf	Body		*	*		BS
cg10360854	5.81E-08	11	124,949,180	*SLC37A2*	−0.28	OpenSea	Body		*		*	BS
5hmC DMPs												
cg00456797	1.36E-03	2	207,233,872		0.16	OpenSea	IGR					
cg20991802	8.13E-03	22	17,724,817		0.12	OpenSea	IGR					
cg13638884	8.13E-03	10	125,223,731		0.12	OpenSea	IGR					BS
cg11385411	1.23E-02	1	184,133,807		0.11	OpenSea	IGR				*	
cg13631605	1.23E-02	6	160,405,572	*IGF2R*	0.12	OpenSea	Body					
cg09550697	1.23E-02	8	145,012,068	*PLEC1*	0.15	S_Shelf	Body		*	*		5mC
cg13388131	1.23E-02	11	62,211,493	*AHNAK*	0.12	N_Shore	Body					
cg19800026	1.23E-02	5	14,492,945	*TRIO*	0.18	OpenSea	Body		*		*	BS
cg01025883	1.23E-02	16	23,867,088	*PRKCB*	0.12	OpenSea	Body		*			
cg27058773	1.58E-02	17	66,309,601	*ARSG*	0.17	OpenSea	Body				*	

Probe: Illumina probe ID; adj.P.Val: Benjamini-Hochberg corrected *P* value (FDR); Chr: Chromosome; Gene: UCSC gene name; Delta Beta: difference in mean β-values between smokers and non-smokers; Island Relation: Relation to CpG Island; Feature: Gene feature; Enh: Identified enhancer in FANTOM5 consortium; 450 k chip: Present on Infinium 450 k BeadChip; Blood: Significant in blood cell DNA methylation smoke signature as previously reported [7]; AMs 450 k; Significant in alveolar macrophages in smokers as previously reported [14]; * indicates presence in database, on chip, or in related studies; DMP overlap: Overlapping with BS (total 5mC + 5hmC), 5mC or 5hmC DMPs.

Please cite this article as: M.V. Ringh, M. Hagemann-Jensen, M. Needhamsen, et al., Tobacco smoking induces changes in true DNA methylation, hydroxymethylation and gene expression in b..., EBioMedicine, https://doi.org/10.1016/j.ebiom.2019.07.006

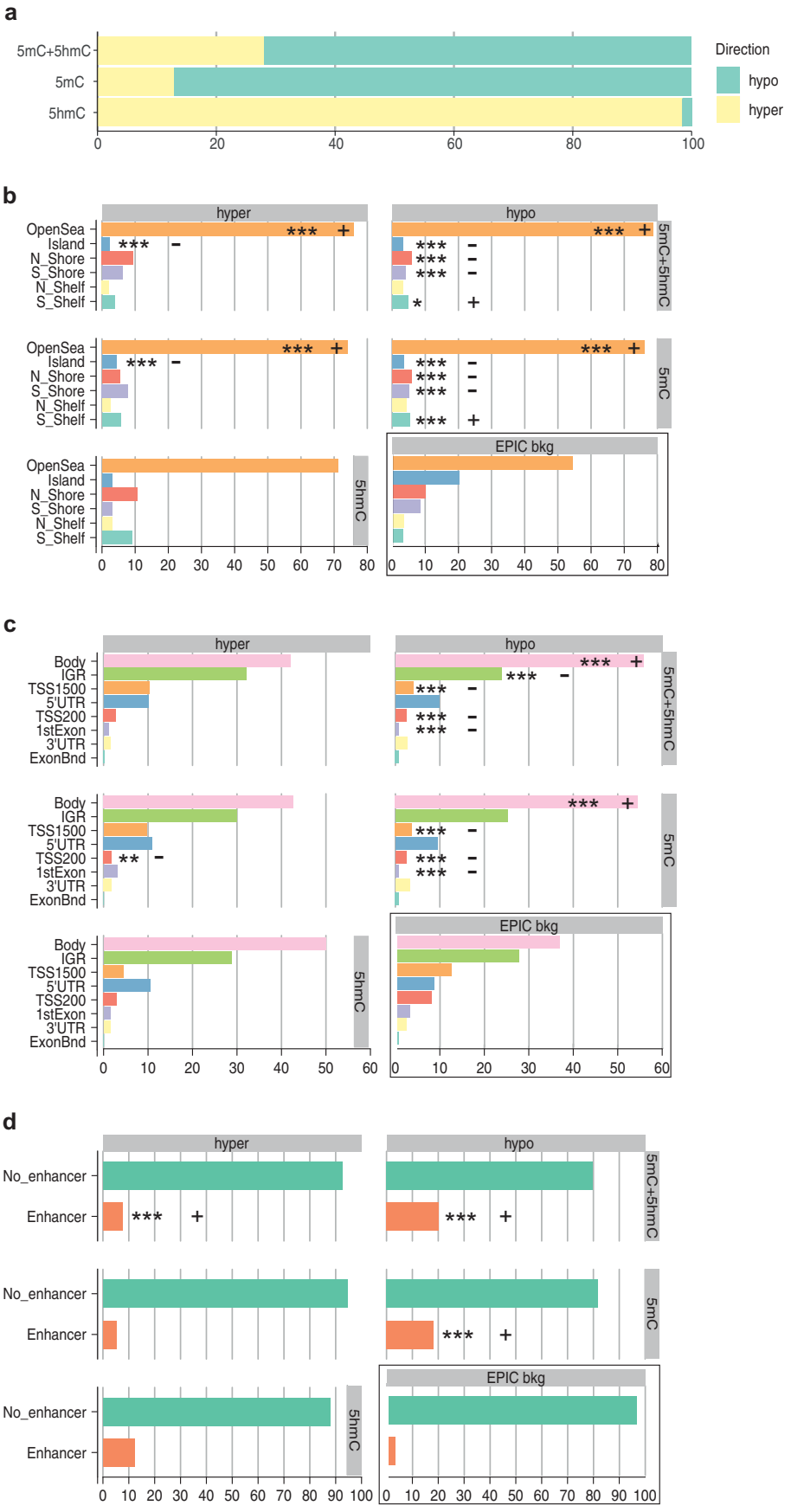

Please cite this article as: M.V. Ringh, M. Hagemann-Jensen, M. Needhamsen, et al., Tobacco smoking induces changes in true DNA methylation, hydroxymethylation and gene expression in b..., EBioMedicine, https://doi.org/10.1016/j.ebiom.2019.07.006

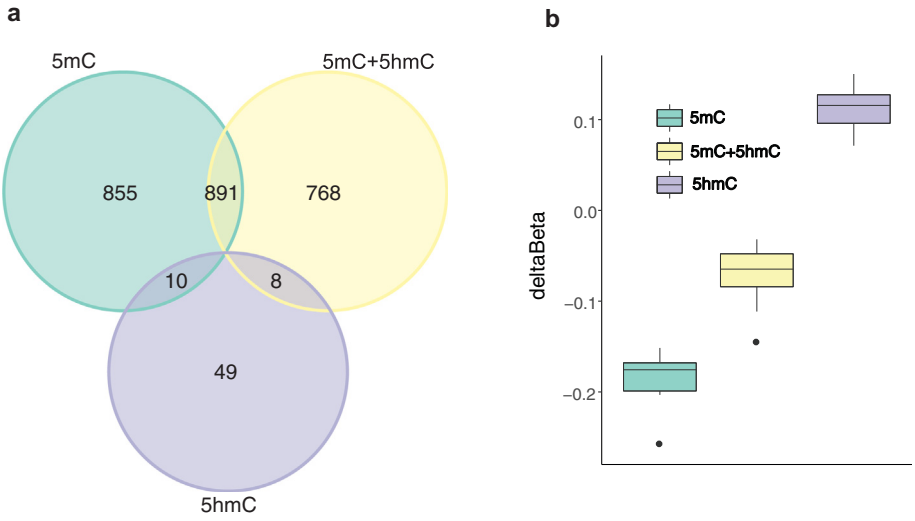

Fig. 3. Hypomethylation and hyperhydroxymethylation in smokers. Overlapping total 5mC + 5hmC (yellow), 5mC (green) and 5hmC (purple) with adjusted *P* value <.05 (absolute Δβ threshold: 5mC + 5hmC and 5mC >0.15; 5hmC >0.05). (**a**) Venn diagram illustrating number of DMPs and overlaps between 5mC + 5hmC, 5mC, and 5hmC. (**b**) Boxplot showing 5mC + 5hmC, 5mC and 5hmC Δβ for the 10 overlapping DMPs between 5mC and 5hmC. (For interpretation of the references to colour in this figure legend, the reader is referred to the web version of this article.)

than the difference in content of alveolar macrophages in BAL of smokers (median = 96.5% compared to median = 90.8% for non-smokers), to exclude potential DMPs that would be caused by a difference in cell proportions alone. Analysis of 5mC + 5hmC and 5mC data from BAL cells revealed 1667 total 5mC + 5hmC DMPs (Table 2; Supplementary Table 2) and 1713 5mC DMPs (Table 2; Supplementary Table 3) associated with smoking (FDR-adjusted P <0.05, absolute Δβ >0.15). 5hmC was quantified by subtracting 5mC β-values from 5mC + 5hmC β-values (735,794) in 35 overlapping BS and oxBS samples from smokers and non-smokers. As expected, 5hmC methylation values ranged at lower level and a minor fraction of probes displayed slightly negative values. We therefore set an absolute Δβ threshold of >0.05 when calling 5hmC and found 67 significant 5hmC DMPs (Table 2; Supplementary Table 4) after correcting for multiple testing (FDR-adjusted P < .05). The most significant 5mC + 5hmC, 5mC, and 5hmC DMPs are shown in Supplementary Fig. 3.

As expected, DNA methylation QQ plots (Supplementary Fig. 4) show inflated observed –log10 *P* values, both after adjusting for covariates (sex+age) and when removing unwanted variables using RUVm [37]. This is not uncommon in EWAS studies [45,46] where alterations in the phenotype also may reflect other underlying factors, unlike genome-wide association studies where a genetic variant is closely linked to a phenotype. In order to investigate statistical power, we performed a post-hoc analysis using a power analysis tool designed specifically for EWAS studies (pwrEWAS). With a sample size of 35 and an effect size (absolute Δβ) of 0.15, the estimated statistical power of the current study is >0.8 (Supplementary Fig. 5), which is a common cut-off for well-powered studies.

Regarding cell composition across individuals, we observed a high proportion of macrophages across our samples (median > 90%). However, BAL from smokers is known to present an increased macrophage fraction and decreased lymphocyte fraction [43], which was also the case in our cohort. We hypotesise that correction for cell type composition might mask some of the impact of smoke exposure since the smoking effect will also be adjusted due to multicollinearity. To test this, we compared our findings with 5mC + 5hmC, 5mC, 5hmC DMP analyses using cell-type as an additional covariate in the linear model while applying the same criteria for significance (FDR-adjusted P < .05) and effect size (5mC + 5hmC and 5mC: absolute Δβ >0.15; 5hmC: absolute Δβ >0.05). Spearman's correlation coefficients (Rho) indicated that there was no overall strong correlation between cell type and DMP β-values (Supplementary Fig. 6, Rho and *P* values has been added to Supplementary Table 2–4). Additionally, the FDR-adjusted *P* values from the cell type-adjusted and unadjusted DMP lists strongly correlated (Supplementary Fig. 7). Given the high proportion of macrophages across our samples, it is likely that our DNA methylation changes are specific to this particular cell type. To address this, we performed eFORGE analyses [39] (based on DNase I hypersensitive sites or DHSs) applied to the top DMPs of total 5mC + 5hmC (1000 probes), 5mC (1000 probes), and 5hmC (67 probes). Since alveolar macrophages are not part of the Epigenome Roadmap [47], we based the overlaps on peripheral blood cell types including monocytes. As expected, eFORGE results (Supplementary Fig. 8) showed that monocytes (primary monocytes in peripheral blood) were by far the most enriched cell type among our DMPs (5mC + 5hmC q-value = 1.77×10^{-152}; 5mC q-value = 1.04×10^{-153}; 5hmC q-value = 1.77×10^{-13}), demonstrating co-localisation of monocyte DHS sites and smoking-associated DMPs. In contrast, we did not see any significant enrichment of T cells (primary T cells from peripheral blood) among our DMPs (5mC + 5hmC q-value = ns; 5mC q-value = ns; 5hmC q-value = ns), further validating that our findings were indeed macrophage-specific.

The majority of the significant DMPs were hypomethylated in smokers compared to non-smokers (Fig. 2a), but to a larger extent in 5mC (87%) than in 5mC + 5hmC (72%), suggesting that a fraction of the 5mC + 5hmC DMPs display 5hmC modification. This is confirmed by the predominant hypermethylation in 5hmC DMPs (Fig. 2a). Next, we stratified the significant DMPs into CGI (Fig. 2b) and gene-related features (Fig. 2c), and performed enrichment analysis relative to the EPIC background (735,794) probe distribution. In summary, analysis of significant DMPs revealed that both 5mC + 5hmC and 5mC hypo-

Fig. 2. Smoking-associated DMPs are predominantly hypomethylated in 5mC and total 5mC + 5hmC with enrichment in gene bodies, non-CGI context and enhancer sites. Horizontal bar plots (**a-d**) illustrating relative frequencies of DMPs associated with smoking. (**a**) Relative frequencies of hypermethylated and hypomethylated 5mC + 5hmC, 5mC, and 5hmC DMPs. Percentage of hypermethylated and hypomethylated 5mC + 5hmC, 5mC and 5hmC across (**b**) CGI-related features (CpG islands, shores, shelves, open sea), (**c**) gene features (TSS1500, TSS200, 1stExon, 5'UTR, Body, 3'UTR, ExonBnd, IGR), and (**d**) enhancers. The distribution of all EPIC array probes included in our analysis are shown as EPIC bkg (background) for comparison (**b-d**). Enrichment/depletion analysis was performed using Chi-square test on frequencies, adjusting *P* values for multiple testing (Bonferroni). * P < .05 compared to non-smokers, ** P < .01 compared to non-smokers, *** P < .001 compared to non-smokers.

Please cite this article as: M.V. Ringh, M. Hagemann-Jensen, M. Needhamsen, et al., Tobacco smoking induces changes in true DNA methylation, hydroxymethylation and gene expression in b..., EBioMedicine, https://doi.org/10.1016/j.ebiom.2019.07.006

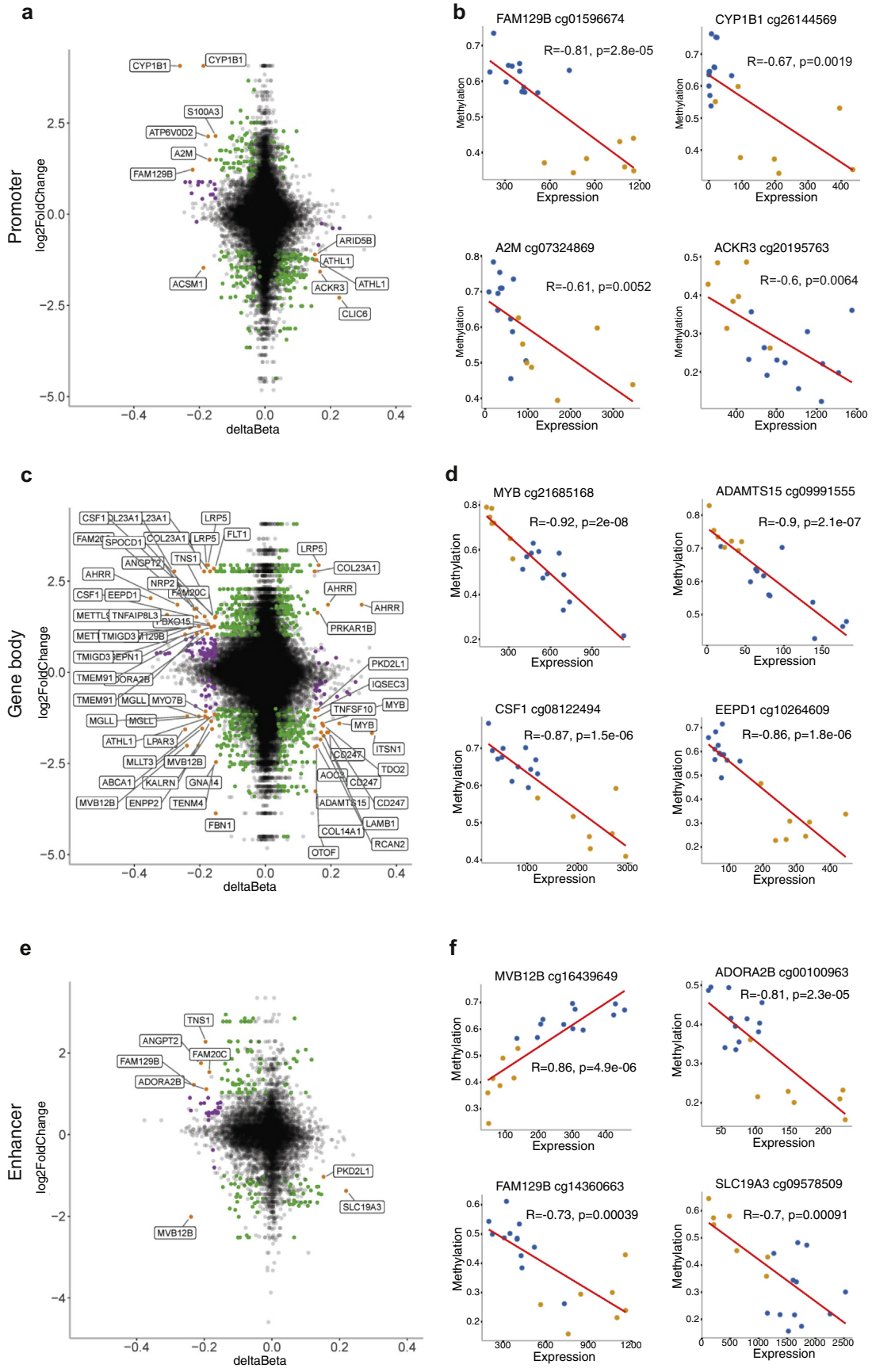
a
Promoter
log2FoldChange
deltaBeta
CYP1B1
S100A3
ATP6V0D2
A2M
FAM129B
ARID5B
ATHL1
ACSM1
ACKR3
CLIC6
b
FAM129B cg01596674
R=-0.81, p=2.8e-05
CYP1B1 cg26144569
R=-0.67, p=0.0019
A2M cg07324869
R=-0.61, p=0.0052
ACKR3 cg20195763
R=-0.6, p=0.0064
Methylation
Expression
c
Gene body
log2FoldChange
deltaBeta
LRP5
COL23A1
AHRR
PRKAR1B
PKD2L1
IQSEC3
MYB
TNFSF10
ITSN1
TDO2
CD247
ADAMTS15
LAMB1
RCAN2
FBN1
COL14A1
OTOF
d
MYB cg21685168
R=-0.92, p=2e-08
ADAMTS15 cg09991555
R=-0.9, p=2.1e-07
CSF1 cg08122494
R=-0.87, p=1.5e-06
EEPD1 cg10264609
R=-0.86, p=1.8e-06
e
Enhancer
log2FoldChange
deltaBeta
TNS1
ANGPT2
FAM20C
FAM129B
ADORA2B
PKD2L1
SLC19A3
MVB12B
f
MVB12B cg16439649
R=0.86, p=4.9e-06
ADORA2B cg00100963
R=-0.81, p=2.3e-05
FAM129B cg14360663
R=-0.73, p=0.00039
SLC19A3 cg09578509
R=-0.7, p=0.00091

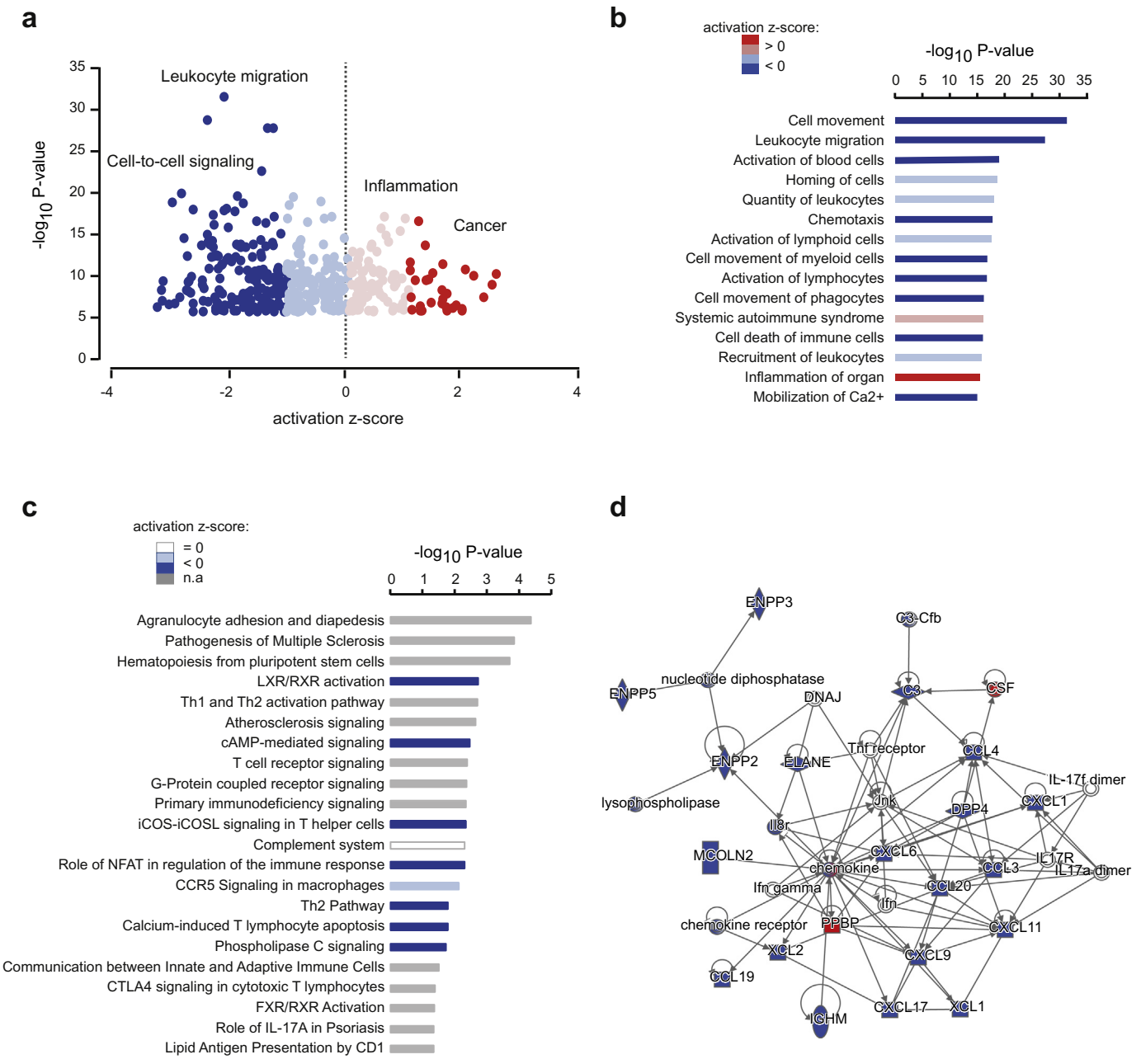

Fig. 5. Functional annotations of differentially expressed genes. All (**a**) and top (**b**) biological processes and diseases associated with differentially expressed genes obtained with Ingenuity Pathway Analysis (IPA). Top canonical pathways (**c**) associated with differentially expressed genes obtained with IPA. (**d**) Schematic representation of the top gene interaction network obtained with IPA, with downregulated and upregulated genes depicted in blue and red, respectively. (**a-c**) Significance is represented as $-\log_{10} P$ value and colours indicate predicted activation z-score, with decreased, no effect, and increased activation in blue, white and red colours respectively. n.a. prediction not available. (For interpretation of the references to colour in this figure legend, the reader is referred to the web version of this article.)

and hypermethylated changes, caused by smoking, predominantly occur in open seas and CGI ($P < .001$). Hypermethylated 5hmC sites (66 DMPs) were also found more often in open sea and underrepresented at CGI, without however, reaching significance level. Hypomethylated 5mC + 5hmC and 5mC DMPs were enriched in gene bodies (Fig. 2c), and depleted in TSS1500, TSS200, and 1st Exon ($P <$ .001). Hypermethylated 5hmC sites were not significantly changed, but followed the same directionality as hypomethylated 5mC, with enrichment at gene bodies and depletion at TSS1500 and TSS200. Interestingly, we found a striking enrichment of both among 5mC + 5hmC and 5mC DMPs in FANTOM5 enhancers (Fig. 2d). This is the case especially for hypomethylated DMPs, with enrichment from 3.3% of total EPIC

Fig. 4. Correlation of promoter, gene body, and enhancer methylation with gene expression. Plots showing genes with differences in both DNA methylation and expression in promoters **(a-b)**, gene body **(c-d)**, and enhancers **(e-f)** of smokers-associated DMPs and genes. Scatterplots of mean gene expression values (log2 fold change) and total methyl (5mC + 5hmC) mean Δβ in promoter (**a**), gene body (**c**), and enhancer (**e**). Orange dots represent genes with significant smoking-associated changes in both total 5mC + 5hmC (>0.15 absolute Δβ) and gene expression (log2 fold change >1), green dots represent significant expression but not methylation, and purple dots represent changes in 5mC + 5hmC but not gene expression **(b,d,f)**. Correlation plots of selected genes showing both methylation (5mC + 5hmC, β-values) and gene expression (normalised gene count), with Pearson correlation coefficient and *P* value **(b,d,f)**. Smokers ($n = 7$) are represented by yellow dots, and ($n = 12$) non-smokers by blue dots. Promoters are represented by TSS200 and TSS1500 CpG sites. Enhancer sites are present at various genomic features and can overlap with both promoter and gene body sites. (For interpretation of the references to colour in this figure legend, the reader is referred to the web version of this article.)

Please cite this article as: M.V. Ringh, M. Hagemann-Jensen, M. Needhamsen, et al., Tobacco smoking induces changes in true DNA methylation, hydroxymethylation and gene expression in b..., EBioMedicine, https://doi.org/10.1016/j.ebiom.2019.07.006

probes (background) to 20.3% of significant 5mC + 5hmC DMPs (244 DMPs, $P < .001$) and 18.1% of 5mC DMPs (276 DMPs, $P < .001$).

Interestingly, only 53% of the true 5mC DMPs (891) overlapped with 5mC + 5hmC DMPs (Fig. 3a), suggesting that relevant changes might be undetected by conventional BS methylation analysis. The 10 overlapping 5mC and 5hmC DMPs (Fig. 3a-b) showed hypomethylated 5mC and hypermethylated 5hmC, further supporting involvement of the DNA demethylation pathway.

Predominant hypomethylation could be further confirmed at region level. In order to do so, we investigated clusters of neighbouring probes for potential differential methylation between smokers and non-smokers, using again a linear model adjusting for age and sex. We focused on differentially methylated regions (DMRs) with clusters of at least two consecutive differentially methylated CpGs and identified 60 5mC + 5hmC and 83 5mC DMRs associated with smoking status at genome-wide level (FDR-adjusted $P < .05$) (Supplementary Table 5 and Supplementary Table 6). In accordance with DMPs analysis, most DMRs were found hypomethylated (90% and 92% of 5mC + 5hmC and 5mC DMRs, respectively).

For technical validation of the EPIC methylation array, we selected a DMP mapping to *ITSN1* (cg11650372), displaying strong hypermethylation in smokers compared to non-smokers. BS and oxBS pyrosequencing confirmed differential methylation in accordance with the EPIC data (BS methyl and 5mC; *P* value <.0001; Supplementary Fig. 9).

3.4. Known and novel smoking-associated DMPs

In order to compare our findings with previously reported DMPs generated using BS-treatment alone, we focused on the 1667 DMPs from total 5mC + 5hmC signals. Strikingly, out of the identified total 1667 DMPs, a substantial fraction (63.8%, 1063 DMPs) were covered only by the EPIC chip (hence absent from previous platforms) (Supplementary Table 2). Among the remaining 604 overlapping probes, 18% (110/604) are known smoking-associated sites from genome-wide studies in blood [7]. In alveolar macrophages, 60% (18/30) of previously

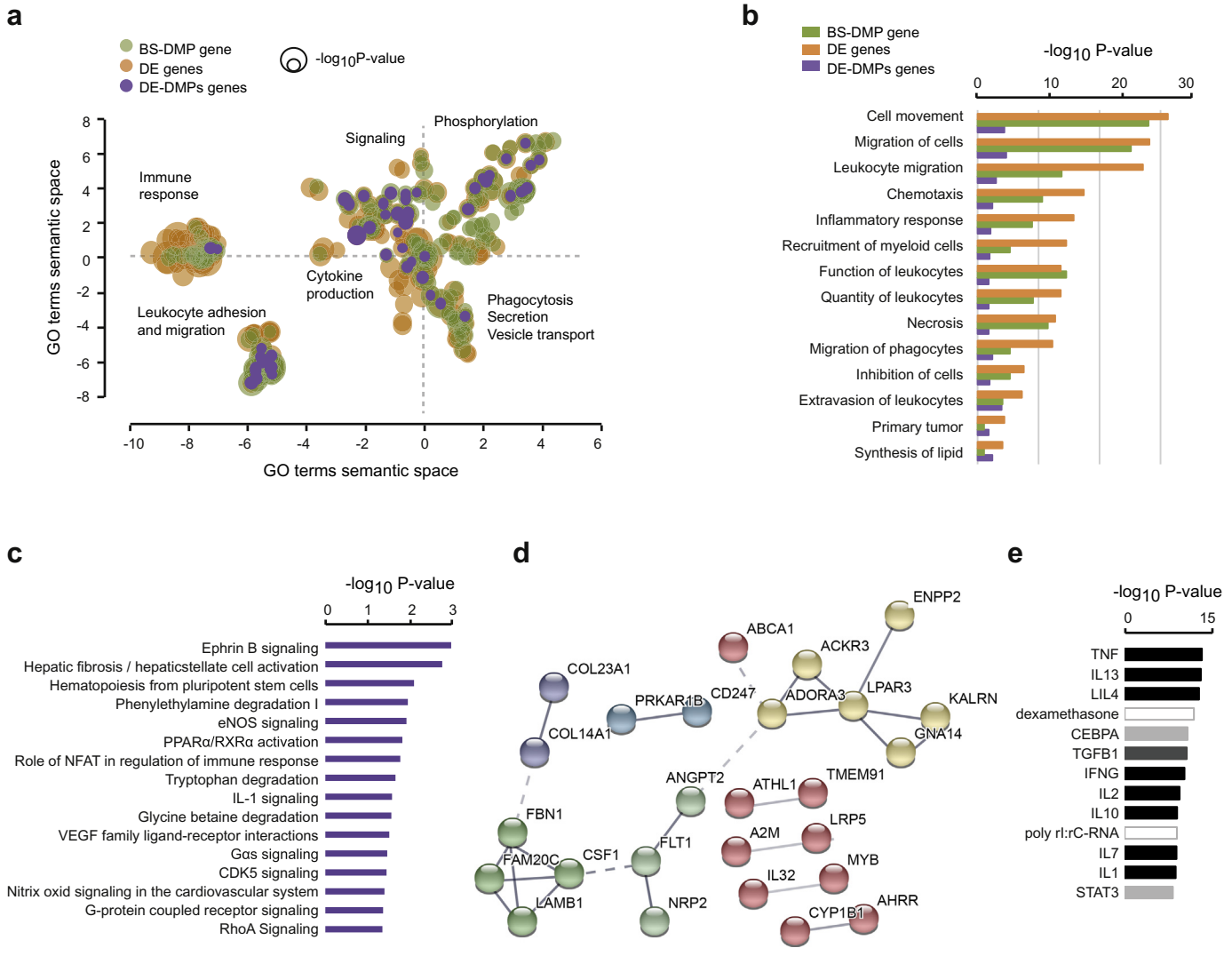

Fig. 6. Functional annotations of differentially methylated and expressed genes. (**a**) Multidimensional scaling of GO Biological processes terms associated with differentially methylated (BS-DMP: total 5mC + 5hmC) (green), differentially expressed (DE) (orange) genes according to semantic similarities. Findings from annotated DE genes that harbour BS-DMPs are depicted in purple. GO terms were obtained using over-representation analysis and visualization was generated by REVIGO. (**b**) Top common biological processes and diseases associated with differentially methylated (BS-DMP) (green) and DE (orange) genes obtained with Ingenuity Pathway Analysis (IPA), with IPA findings from genes displaying both BS-DMP (FDR < 0.05, $\Delta\beta > 0.15$) and transcriptional change in purple. (**c**) Top canonical pathways associated to both DE- and DMP-genes. (**d**) Representation of the genes network obtained with IPA on both DE- and DMP-genes and visualised using STRING. Grey line gradient and thickness indicates the strength of data support (darker thick grey representing stronger confidence) and colours represent different cluster (Markov Clustering set at 6). (**e**) Top upstream regulators for both differentially methylated and expressed genes, with colours depicting different classes of regulators. Significance is represented as $-\log_{10} P$ value. DE, differentially expressed, BS-DMPs, bisulphite-generated differentially methylated positions (5mC + 5hmC). (For interpretation of the references to colour in this figure legend, the reader is referred to the web version of this article.)

Please cite this article as: M.V. Ringh, M. Hagemann-Jensen, M. Needhamsen, et al., Tobacco smoking induces changes in true DNA methylation, hydroxymethylation and gene expression in b..., EBioMedicine, https://doi.org/10.1016/j.ebiom.2019.07.006

reported DMPs [14] were also found significant in our cohort. Seven of our DMPs overlapped with smoking-associated DMPs in both blood cells and alveolar macrophages and map to the *SRGAP1* (cg01668352), *AHRR* (cg25648203), *SUSD4* (cg25466245), *DAB2* (cg17576603), *FGR* (cg11254522), *CD80* (cg13458803) and *RYBP* (cg09006487) genes, respectively.

The most significant 5mC + 5hmC DMP map to the antioxidant-producing *SEPN1* gene (cg04857037, adjusted *P* value = 3.77×10^{-12}), and is specific to the EPIC bead array (Table 2; Supplementary Table 2). The most significant 5mC DMP (Table 2; Supplementary Table 3) was annotated to *TNFAIP8L3* (cg02233197, adjusted *P* value = $2.39\text{Ex}10^{-9}$), and has been previously reported in alveolar macrophages [14], while the most significant 5hmC DMP (cg00456797, adjusted *P* value = 1.85×10^{-3}) is intergenic and specific to the EPIC bead array (Table 2; Supplementary Table 4). Overall, 30% of the 5mC + 5hmC, 50% of the 5mC and 70% of 5hmC top 10 DMPs were specific to the EPIC chip.

3.5. Differential variability of total 5mC + 5hmC and 5mC associated to smoking

Next, we tested whether DNA methylation variability was significantly associated with cigarette smoking. Group-wise analyses of differential variability on M-values revealed 19 significant 5mC + 5hmC differentially variable positions (DVPs) (Supplementary Table 7) and 3 significant 5mC DVPs (Supplementary Table 8) with an FDR-adjusted $P < .05$. The commonly known smoking-associated *AHRR* CpG site cg05575921 was among the top 5mC + 5hmC DVPs, together with CpG site in the bidirectional promoter of oncogene *BRCA1* and the *NBR2* gene (cg20760063). Out of the 3 significant 5mC DVPs, 2 were annotated to the 3'UTR region of *NFYA* (cg06671660, cg09580153).

3.6. Changes in methylation correlate with transcriptional differences

To determine whether the total DNA methylation profiles were associated with differentially expressed genes, RNA was simultaneously extracted from BAL cells from the same individuals and subjected to RNA sequencing (RNA-seq). After filtering reads passing quality threshold (RIN >7, total read count >10), a total of 633 genes were differentially expressed between smokers and non-smokers with an adjusted *P* value <.05 and absolute log2-fold change >1 (Supplementary Table 9).

Since DNA methylation in promoters and gene bodies often correlate with gene regulation, and given the considerable evidence of interactions between enhancers and promoters with subsequent transcriptional regulation [48], we sought to investigate associations between methylation and expression specifically in these regions. We thus focused on all probes annotated to promoter regions (defined here as TSS200 or TSS1500), gene bodies, and enhancer sites. Comparison of 5mC + 5hmC and gene expression changes in smokers vs non-smokers revealed 60 differentially expressed genes, with 90 DMPs annotated to them. A large fraction, 75.5% (68/90), of these 5mC + 5hmC β-values correlated with gene expression (Pearson correlation, $R > 0.5$) (Supplementary Table 10). More specifically, in promoters, a total of 10 differentially expressed genes also showed 5mC + 5hmC changes (12 DMPs) (Fig. 4a). 66.7% (8/12 DMPs) of these genes displayed a negative correlation ($R > 0.5$) between DNA promoter methylation and gene expression, as is often the case with promoter methylation. Smoking associated with hypomethylation and upregulation of 5 genes, including *FAM129B, CYP1B1,* and *A2M* (Fig. 4b), along with hypermethylation and downregulation of 4 genes, such as *ACKR3* and *ATHL1*. An additional 45 genes showed significant differences in both gene body total DNA methylation (63 5mC + 5hmC DMPs) outside of promoter region, and gene expression (Fig. 4c-d), including *MYB*, *EEPD1*, *FLT1*, and the antioxidant-producing *SEPN1*. Interestingly, gene bodies include both hypo- and hypermethylation as well as over- and under-expression, supporting a mechanistic difference between promoters and gene bodies. Enhancer-associated DMPs negatively correlated with gene expression and were mostly located at gene bodies (87.5%, 7/8) including the *MVB12B, ADORA2B*, and *FAM129B* genes (Fig. 4e-f). Overall, 5mC methylation and gene expression associations largely overlapped with 5mC + 5hmC, but included additional genes such as *IL4I1*, *NFIA* (Supplementary Fig. 10a-c), and selectin L-producing *SELL*. A few 5hmC DMPs were also differentially expressed, including *XYLT1*, *SH3RG1*, and *CDA* (Supplementary Fig. 10d-e).

3.7. DNA methylation and expression changes associate with genes involved in immune cells migration and activation

To gain insight into biological functions associated with transcriptional changes in BAL cells from smokers, we performed Ingenuity Pathway analysis (IPA) on the 633 differentially expressed genes (adj. *P* value <.05, log2-fold change >1). Enriched biological functions associated with transcriptional changes showed inhibition of processes such as cellular movement and cell-to-cell signalling while inflammatory response and cancer-related processes were predicted to be activated (Fig. 5a). This is exemplified by the most significant biological functions implicating decreased activity of immune cell chemotaxis, movement and activation (Fig. 5b). The most enriched canonical pathways (Fig. 5c) showed alteration of LXR/RXR activation pathway involved in lipid metabolism and inflammation (Fig. 5d), adhesion and diapedesis of mononuclear leukocytes pathway, a key event in the process of inflammation, and complement system pathway bridging the innate and acquired immune systems, including cell killing, clearance of immune complexes and apoptotic cells and activation of inflammation.

Interestingly, biological processes (GO terms) associated with 5mC + 5hmC DMP-annotated genes strongly overlap with the differentially expressed genes, and differentially expressed genes harbouring DMPs also clusters with them (Fig. 6a). Top biological functions for both differentially methylated and expressed genes converge to immune-related processes such as leukocyte recruitment, migration and adhesion (Fig. 6a-b). Of note, functions and pathways of genes annotated by novel EPIC smoking-associated DMPs converge to similar GO terms as the ones from genes annotated with known (450 K) smoking-associated DMPs (Supplementary Fig. 11). IPA analysis of dysregulated genes affected by 5mC + 5hmC DMPs shows enrichment of canonical pathways related to haematopoiesis, angiogenesis, immune/oxidative pathways and metabolism (Fig. 6c), cores genes segregating into functional groups of interconnected genes (Fig. 6d). Among them, *AHRR* and *CYP1B1* are known genes involved in AHR detoxification pathway. Likewise, genes showing DNA methylation and transcriptional changes have common upstream regulators, most of which are cytokines typically found in an inflammatory milieu, such as the pro-inflammatory TNF, IFN-γ and IL-1 and the anti-inflammatory IL-4 and IL-10 cytokines. Thus, smoking-associated changes in DNA methylation and gene expression alter genes important for immune functions of BAL cells.

Overall, we found a major overlap of 5mC + 5hmC and 5mC (Supplementary Table 11), suggesting that 5mC accounts for a substantial fraction of the biological terms for pathway analysis. Regarding 5hmC as a separate modification, there was not enough significant DMPs at FDR-adjusted *P* value <.05 to perform pathway analysis. As an exploratory step, we performed analysis on DMPs at an unadjusted *P* value <.001 (1659 DMPs, Supplementary Table 11). Even though these findings should be interpreted with caution, they reveal that the large majority (80%) of canonical pathways associated to candidate 5hmC DMPs overlap with 5mC DMPs.

3.8. Transcription factor analysis

The monocyte-specific signature of the DMPs (Supplementary Fig. 8), indicates that these probes point to regulatory elements present in cells from the monocyte/macrophage line rather than T cells or B cells. DHSs can include several classes of regulatory elements, including

Please cite this article as: M.V. Ringh, M. Hagemann-Jensen, M. Needhamsen, et al., Tobacco smoking induces changes in true DNA methylation, hydroxymethylation and gene expression in b..., EBioMedicine, https://doi.org/10.1016/j.ebiom.2019.07.006

promoters, enhancers, and CTCF-binding sites. In order to refine our previous associations, we performed further analyses with chromatin states (defined by the Epigenomics Roadmap Project [47]) on the same 5mC + 5hmC and 5mC DMPs and found monocyte/macrophage enhancers as the top category, suggesting that the DHS enrichment is driven mainly by overlap with monocyte/macrophage enhancers. To gain more insight into the molecular processes involved in the observed smoking response signature, we performed eFORGE-TF (transcription factor) analysis and identified several significant TF motif associations with both the 5mC + 5hmC and 5mC DMPs. Similar TF motifs were found for 5mC + 5hmC (Supplementary Fig. 12; Supplementary Table 12) and 5mC DMPs (Supplementary Fig. 13; Supplementary Table 13). Using PANTHER pathway analysis, genes associated with these TF motifs revealed the platelet derived growth factor (PDGF) signalling pathway as the top enriched pathway (Fold enrichment: 14.55, *P* value: 2.74×10^{-2}). Thus, eFORGE-TF and PANTHER analyses of differentially methylated changes in BAL macrophages link smoking with the PDGF signalling pathway.

4. Discussion

We have investigated DNA modifications and gene expression in alveolar macrophage-enriched bronchoalveolar lavage cells from healthy smokers and non-smokers. This is, to our knowledge, the first report of smoking-associated genome-wide methylation data in pulmonary cells that includes true 5mC and 5hmC as separate modifications, especially in combination with the EPIC BeadChip. We identified a large number of smoking-associated DMPs (5mC + 5hmC, 1667; 5mC, 1713; 5hmC, 67), many of them located in enhancers. Our findings suggest that smoking-associated differences may include DNA demethylation of 5mC with a 5hmC intermediate, an interpretation based on the detected opposing hypomethylated 5mC and hypermethylated 5hmC data. Importantly, we could correlate our DNA methylation data with gene expression, and associate tobacco smoking with genes involved in cancer, immune cell migration, and activation pathways. The observed smoking-associated effect on DNA methylation and gene expression in BAL cells is likely to have implications on disease risk of several pathologies such as cancer, COPD, and autoimmune diseases.

In this study, we do not only show that tobacco smoking induce alterations in 5mC + 5hmC and gene expression in BAL cells from healthy individuals, but also report significant changes in 5hmC. It has been well-established that oxidative stress (ROS) underlying smoke-related lung inflammation, results in DNA damage and cytotoxic events [49]. For example, the oxidative damage biomarker 8-oxoG, is significantly elevated in lung tissue of smokers and also correlates with number of cigarettes smoked per day [25]. The DNA demethylation system catalysed by the TET enzymes also appears to be regulated by oxidative state, where oxidative stress may lead to demethylation initiated by TET enzymes [22]. This may induce formation of 5hmC but could importantly also lead to active continuous oxidation to formyl and carboxyl, which would actually lower the amount of 5hmC. Since 8-oxoG is essential for initiation of oxidative stress-induced DNA demethylation [22] and is abundant in smokers [25,49], we would expect to see many hypomethylated 5mC DMPs in smokers compared to nonsmokers. Interestingly, nearly all of the 67 identified 5hmC DMPs were hypermethylated while most of the 5mC + 5hmC and 5mC top DMPs, DVPs and DMRs were hypomethylated. This association supports the hypothesis that smoking can promote demethylation by oxidation of 5mC into 5hmC, a modification that can also exert effect as a stable mark. Future studies are warranted to decipher the mechanisms underlying the methylation profiles observed in BAL cells from smokers in general, and the contribution of oxidative stress-related 8-oxoG in such processes.

DNA demethylation of 5mC into 5hmC may also lead to functional effects, since these modifications have distinct properties such as different affinity to transcription factors [23]. In contrast to 5mC, which is able to bind transcriptional repressors, 5hmC can inhibit this binding and thereby counteract the repressive effect of 5mC [21]. While 5mC is often associated with gene repression, 5hmC facilitates transcription by contributing to an open chromatin state [21]. This has been widely studied in adult neurons and during embryogenesis where there is a relatively high abundance of 5hmC. For example, in mouse embryonic stem cells, the majority of 5hmC are located in gene bodies, and associated with moderate CpG density [50]. In our study, 5hmC is mainly located in highly methylated regions such as 3'UTR, 5'UTR, gene bodies, exon boundaries, and intergenic regions, and this is also where most smoking-associated 5hmC DMPs are observed. It should also be noted that while the hydroxymethylation results of the current study are highly interesting and novel, they also need to be replicated in future studies.

CpG sites associated with the aryl hydrocarbon receptor repressor (*AHRR*) gene often appear as top significantly differentially methylated in studies on the effect of smoking [7,10,13]. This is the case in our cohort as well, where three 5mC + 5hmC and six 5mC DMPs were annotated to *AHRR*, along with one 5mC + 5hmC DVP. The aryl hydrocarbon pathway regulates cytochrome P450 family members, metabolic enzymes involved in the elimination of xenobiotics that may have entered the body through i.e. the lungs. One group of xenobiotics includes the polycyclic aromatic hydrocarbons (PAH), which are increased in the lung tissue of tobacco smokers [51]. Many of these PAHs are carcinogenic and are, after metabolic activation, able to bind to DNA bases and form DNA adducts that in turn can lead to mutations in oncogenes and tumour suppressor genes [51]. The AhR-dependent cytochrome P450 family member 1B1 (*CYP1B1*), another differentially methylated gene in our study, is highly induced by PAHs, and responsible for metabolising many xenobiotics, including metabolic activation of PAH [52]. In addition, CYP1B1 also metabolizes many physiological compounds, including steroid hormones such as testosterone and oestrogen. Noteworthy, CYP1B1 is involved in both hydroxylation and demethylation of oestrogen products, and the rapid oxidation of 4-hydroxylated oestrogens to quinones [53,54]. This redox recycling leads to ROS production and oxidative DNA damage, which may lead to DNA adduct formation and carcinogenesis [54,55].

In our study, we found several hypomethylated promoter DMPs in genes from smokers that associate with increased gene expression, one of them being *CYP1B1*. Previous studies of smokers have reported upregulated *CYP1B1* expression in the oral mucosa [56] and bronchial airway epithelium [57]. Due to the direct contact between alveolar macrophages and lung tissue, the hypomethylated promoter of *CYP1B1* in combination with the increased expression, may have a significant role in the activation of procarcinogens and biotransformation to carcinogens. Functional phagocytic capacity is highly relevant for alveolar macrophages and this was impaired in a study on *CYP1B1*-deficient mice, suggesting a role for *CYP1B1* in clearance of debris [58], and an attempt to increase this capacity as a response to smoking. Genome-wide epigenetic studies have emphasised that the location of DNA methylation in relation to the gene, influences the direction of gene expression. For example, DNA methylation occurring in promoter regions of genes, is well known to repress gene expression [59]. In gene bodies on the other hand, DNA methylation does not inhibit transcription and might even be positively correlated with expression [15]. Interestingly, it has been shown that AhR can bind to the promoter region (TSS1500) of *CYP1B1* [60], the same region we found hypomethylated both at DMP and DMR level in our study.

Enhancer–promoter interaction through spatial chromatin organisation is a fundamental part of transcriptional regulation [48]. Enhancers are located at various distances from promoters and contain binding sites for sequence-specific transcription factors, and compared to promoters, enhancer usage varies vastly across cell types [61]. Tissue-resident macrophages, such as alveolar macrophages, exhibit distinct enhancer landscapes that are influenced by the tissue microenvironment in which they reside [61]. In the present study, we observed a

Please cite this article as: M.V. Ringh, M. Hagemann-Jensen, M. Needhamsen, et al., Tobacco smoking induces changes in true DNA methylation, hydroxymethylation and gene expression in b..., EBioMedicine, https://doi.org/10.1016/j.ebiom.2019.07.006

large enrichment of hypomethylated DMPs annotated to enhancers, suggesting that these sites are highly affected by smoking exposure. Investigation of transcription factor motifs enriched for our DMPs identified the PDGF signalling pathway, a mediator of vascular remodelling that may be implicated in cigarette smoke-induced pulmonary artery hypertension [62].

Pathway analysis of transcriptional changes in our study revealed biological functions highly relevant to well-known smoking-related disease processes. We identified inhibition of biological processes such as cellular movement, migration and adhesion and cell-to-cell signalling, while inflammatory response and cancer-related processes showed increased activity. Interestingly, the most enriched canonical pathway is related to LXR/RXR activation with involvement in lipid metabolism and inflammation. In support of this, our highly significant DMP and gene expression top hit *EEPD1* has recently been identified as a LXR target gene, proposed to promote cellular cholesterol efflux in macrophages, by controlling *ABCA1* activity and protein levels [63]. Additionally *EEPD1* has recently been characterised as a protein being recruited to stalled replication forks during replication stress, where it promotes restart of the replication fork [64]. Since smoking is known to damage DNA, and thereby create barriers for DNA replication, the upregulated *EEPD1* expression seen in BAL cells could therefore be a response to the replication fork stress.

By combining methylome and transcriptome data from BAL cells, our study provides new insights into the biological impact of smoking locally in the lungs and possibly systemically in peripheral immune functions. Our findings confirm previously reported DNA methylation and gene expression results from alveolar macrophages, but also reveal new smoking-associated signatures. These novel targets especially map to regions that have not been covered with the previous methodologies, thus increasing and refining our knowledge of the molecular mechanisms underlying the effect of smoking.

Supplementary data to this article can be found online at https://doi.org/10.1016/j.ebiom.2019.07.006.

Acknowledgments

We thank all the volunteers contributing to the study. We would also like to thank Heléne Blomqvist, Margitha Dahl, and Gunnel de Forest for recruitment and management of volunteers, and Benita Engvall for sample handling. We also thank the Uppsala Multidisciplinary Centre for Advanced Computational Science (UPPMAX; Uppsala University) for computational resources.

Funding sources

This study was supported by the Swedish Research Council (MH-2012-13; 2016–01209), the Swedish Heart-Lung Foundation (20120448; 20140666; 20150559; 20160300), the regional agreement on medical training and clinical research (ALF) between Stockholm County Council and Karolinska Institutet, The King Gustav's and Queen Victoria's Freemasons' Foundation, Knut and Alice Wallenberg Foundation (grant number KAW 201.0148), Neuro Sweden, and the Swedish MS foundation. The funders had no role in the design of the study, data collection, data analysis, interpretation, or the writing of this report. The corresponding authors had access to all the data in the study and had final responsibility for the decision to submit for publication.

Declaration of interests

The authors declare that they have no competing interests.

Author contributions

M.V.R., M.H-J., J.Ö. and T.J.E. conceptualised and designed the study. M.V.R. conducted DNA methylation experiments and M.H-J extracted DNA/RNA and performed RNA-seq experiments. M.V.R. performed the main data and statistical analysis, and M.N. and L.K contributed with input and interpretation. M.H-J and Y.L. performed RNA-seq analysis and L.K. conducted IPA analysis. L.K.S. and L.S. performed pyrosequencing analysis. C.B. performed transcription factor analysis. J.W., J.G., B.B., designed and/or contributed to the collection of patient samples. S.K. performed BAL and characterised study subjects. M.J., M.A., J.Ö., and T.J.E. supervised the work in each contributing research group. M.V.R. and T.J.E. initiated the study and wrote the manuscript with contribution from L.K., M.N, M.H-J., and M.J. All authors read and approved the final manuscript.

References

[1] Ezzati M, Lopez AD. Estimates of global mortality attributable to smoking in 2000. Lancet 2003;362(9387):847–52.
[2] Kallberg H, Ding B, Padyukov L, Bengtsson C, Ronnelid J, Klareskog L, et al. Smoking is a major preventable risk factor for rheumatoid arthritis: estimations of risks after various exposures to cigarette smoke. Ann Rheum Dis 2011;70(3):508–11.
[3] Hedstrom AK, Sundqvist E, Baarnhielm M, Nordin N, Hillert J, Kockum I, et al. Smoking and two human leukocyte antigen genes interact to increase the risk for multiple sclerosis. Brain 2011;134:653–64 Pt 3.
[4] Rodgman A, Perfetti TA. The chemical components of tobacco and tobacco smoke. . 2nd Edition ed.Boca Raton: CRC Press; 2013.
[5] Hussell T, Bell TJ. Alveolar macrophages: plasticity in a tissue-specific context. Nat Rev Immunol 2014;14(2):81–93.
[6] Lee J, Taneja V, Vassallo R. Cigarette smoking and inflammation: cellular and molecular mechanisms. J Dent Res 2012;91(2):142–9.
[7] Joehanes R, Just AC, Marioni RE, Pilling LC, Reynolds LM, Mandaviya PR, et al. Epigenetic signatures of cigarette smoking. Circ Cardiovasc Genet 2016;9(5):436–47.
[8] Breitling LP, Yang R, Korn B, Burwinkel B, Brenner H. Tobacco-smoking-related differential DNA methylation: 27K discovery and replication. Am J Hum Genet 2011;88(4):450–7.
[9] Ambatipudi S, Cuenin C, Hernandez-Vargas H, Ghantous A, Le Calvez-Kelm F, Kaaks R, et al. Tobacco smoking-associated genome-wide DNA methylation changes in the EPIC study. Epigenomics 2016;8(5):599–618.
[10] Marabita F, Almgren M, Sjoholm LK, Kular L, Liu Y, James T, et al. Smoking induces DNA methylation changes in multiple sclerosis patients with exposure-response relationship. Sci Rep 2017;7(1):14589.
[11] Joubert BR, Haberg SE, Nilsen RM, Wang X, Vollset SE, Murphy SK, et al. 450K epigenome-wide scan identifies differential DNA methylation in newborns related to maternal smoking during pregnancy. Environ Health Perspect 2012;120(10):1425–31.
[12] Joubert BR, Felix JF, Yousefi P, Bakulski KM, Just AC, Breton C, et al. DNA methylation in Newborns and maternal smoking in pregnancy: genome-wide consortium meta-analysis. Am J Hum Genet 2016;98(4):680–96.
[13] Philibert RA, Sears RA, Powers LS, Nash E, Bair T, Gerke AK, et al. Coordinated DNA methylation and gene expression changes in smoker alveolar macrophages: specific effects on VEGF receptor 1 expression. J Leukoc Biol 2012;92(3):621–31.
[14] Monick MM, Beach SR, Plume J, Sears R, Gerrard M, Brody GH, et al. Coordinated changes in AHRR methylation in lymphoblasts and pulmonary macrophages from smokers. Am J Med Genet B Neuropsychiatr Genet 2012;159B(2):141–51.
[15] Jones PA. Functions of DNA methylation: islands, start sites, gene bodies and beyond. Nat Rev Genet 2012;13(7):484–92.
[16] Li E, Zhang Y. DNA methylation in mammals. Cold Spring Harb Perspect Biol 2014;6(5):a019133.
[17] Tahiliani M, Koh KP, Shen Y, Pastor WA, Bandukwala H, Brudno Y, et al. Conversion of 5-methylcytosine to 5-hydroxymethylcytosine in mammalian DNA by MLL partner TET1. Science 2009;324(5929):930–5.
[18] He YF, Li BZ, Li Z, Liu P, Wang Y, Tang Q, et al. Tet-mediated formation of 5-carboxylcytosine and its excision by TDG in mammalian DNA. Science 2011;333(6047):1303–7.
[19] Ito S, Shen L, Dai Q, Wu SC, Collins LB, Swenberg JA, et al. Tet proteins can convert 5-methylcytosine to 5-formylcytosine and 5-carboxylcytosine. Science 2011;333(6047):1300–3.
[20] Jin SG, Wu X, Li AX, Pfeifer GP. Genomic mapping of 5-hydroxymethylcytosine in the human brain. Nucleic Acids Res 2011;39(12):5015–24.
[21] Mendonca A, Chang EH, Liu W, Yuan C. Hydroxymethylation of DNA influences nucleosomal conformation and stability in vitro. Biochim Biophys Acta 2014;1839(11):1323–9.
[22] Zhou X, Zhuang Z, Wang W, He L, Wu H, Cao Y, et al. OGG1 is essential in oxidative stress induced DNA demethylation. Cell Signal 2016;28(9):1163–71.
[23] Menezo YJ, Silvestris E, Dale B, Elder K. Oxidative stress and alterations in DNA methylation: two sides of the same coin in reproduction. Reprod BioMed Online 2016;33(6):668–83.
[24] Nestor C, Ruzov A, Meehan R, Dunican D. Enzymatic approaches and bisulfite sequencing cannot distinguish between 5-methylcytosine and 5-hydroxymethylcytosine in DNA. Biotechniques 2010;48(4):317–9.
[25] Asami S, Manabe H, Miyake J, Tsurudome Y, Hirano T, Yamaguchi R, et al. Cigarette smoking induces an increase in oxidative DNA damage, 8-hydroxydeoxyguanosine, in a central site of the human lung. Carcinogenesis 1997;18(9):1763–6.

Please cite this article as: M.V. Ringh, M. Hagemann-Jensen, M. Needhamsen, et al., Tobacco smoking induces changes in true DNA methylation, hydroxymethylation and gene expression in b..., EBioMedicine, https://doi.org/10.1016/j.ebiom.2019.07.006

[26] Olsen HH, Grunewald J, Tornling G, Skold CM, Eklund A. Bronchoalveolar lavage results are independent of season, age, gender and collection site. PLoS One 2012;7(8):e43644.
[27] Ockinger J, Hagemann-Jensen M, Kullberg S, Engvall B, Eklund A, Grunewald J, et al. T-cell activation and HLA-regulated response to smoking in the deep airways of patients with multiple sclerosis. Clin Immunol 2016;169:114–20.
[28] Picelli S, Faridani OR, Bjorklund AK, Winberg G, Sagasser S, Sandberg R. Full-length RNA-seq from single cells using Smart-seq2. Nat Protoc 2014;9(1):171–81.
[29] Picelli S, Bjorklund AK, Reinius B, Sagasser S, Winberg G, Sandberg R. Tn5 transposase and tagmentation procedures for massively scaled sequencing projects. Genome Res 2014;24(12):2033–40.
[30] Aryee MJ, Jaffe AE, Corrada-Bravo H, Ladd-Acosta C, Feinberg AP, Hansen KD, et al. Minfi: a flexible and comprehensive Bioconductor package for the analysis of Infinium DNA methylation microarrays. Bioinformatics 2014;30(10):1363–9.
[31] Fortin JP, Triche Jr TJ, Hansen KD. Preprocessing, normalization and integration of the Illumina HumanMethylationEPIC array with minfi. Bioinformatics 2017;33(4):558–60.
[32] Tian Y, Morris TJ, Webster AP, Yang Z, Beck S, Feber A, et al. ChAMP: updated methylation analysis pipeline for Illumina BeadChips. Bioinformatics 2017;33(24):3982–4.
[33] Maksimovic J, Gordon L, Oshlack A. SWAN: subset-quantile within array normalization for illumina infinium HumanMethylation450 BeadChips. Genome Biol 2012;13(6):R44.
[34] Pidsley R, Zotenko E, Peters TJ, Lawrence MG, Risbridger GP, Molloy P, et al. Critical evaluation of the Illumina MethylationEPIC BeadChip microarray for whole-genome DNA methylation profiling. Genome Biol 2016;17(1):208.
[35] Chen H, Boutros PC. VennDiagram: a package for the generation of highly-customizable Venn and Euler diagrams in R. BMC Bioinformatics 2011;12:35.
[36] Du P, Zhang X, Huang CC, Jafari N, Kibbe WA, Hou L, et al. Comparison of Beta-value and M-value methods for quantifying methylation levels by microarray analysis. BMC Bioinformatics 2010;11:587.
[37] Maksimovic J, Gagnon-Bartsch JA, Speed TP, Oshlack A. Removing unwanted variation in a differential methylation analysis of Illumina HumanMethylation450 array data. Nucleic Acids Res 2015;43(16):e106.
[38] Peters TJ, Buckley MJ, Statham AL, Pidsley R, Samaras K, R VL, et al. De novo identification of differentially methylated regions in the human genome. Epigenetics Chromatin 2015;8:6.
[39] Breeze CE, Paul DS, van Dongen J, Butcher LM, Ambrose JC, Barrett JE, et al. eFORGE: a tool for identifying cell type-specific signal in Epigenomic data. Cell Rep 2016;17(8):2137–50.
[40] Zhang B, Kirov S, Snoddy J. WebGestalt: an integrated system for exploring gene sets in various biological contexts. Nucleic Acids Res 2005;33(Web Server):W741–8.
[41] Supek F, Bosnjak M, Skunca N, Smuc T. REVIGO summarizes and visualizes long lists of gene ontology terms. PLoS One 2011;6(7):e21800.
[42] Graw S, Henn R, Thompson JA, Koestler DC. pwrEWAS: a user-friendly tool for comprehensive power estimation for epigenome wide association studies (EWAS). BMC Bioinformatics 2019;20(1):218.
[43] Karimi R, Tornling G, Grunewald J, Eklund A, Skold CM. Cell recovery in bronchoalveolar lavage fluid in smokers is dependent on cumulative smoking history. PLoS One 2012;7(3):e34232.
[44] Globisch D, Munzel M, Muller M, Michalakis S, Wagner M, Koch S, et al. Tissue distribution of 5-hydroxymethylcytosine and search for active demethylation intermediates. PLoS One 2010;5(12):e15367.
[45] Rask-Andersen M, Martinsson D, Ahsan M, Enroth S, Ek WE, Gyllensten U, et al. Epigenome-wide association study reveals differential DNA methylation in individuals with a history of myocardial infarction. Hum Mol Genet 2016;25(21):4739–48.
[46] Liang L, Willis-Owen SAG, Laprise C, Wong KCC, Davies GA, Hudson TJ, et al. An epigenome-wide association study of total serum immunoglobulin E concentration. Nature 2015;520(7549):670–4.
[47] Roadmap Epigenomics C, Kundaje A, Meuleman W, Ernst J, Bilenky M, Yen A, et al. Integrative analysis of 111 reference human epigenomes. Nature 2015;518(7539):317–30.
[48] Mora A, Sandve GK, Gabrielsen OS, Eskeland R. In the loop: promoter-enhancer interactions and bioinformatics. Brief Bioinform 2016;17(6):980–95.
[49] Schieber M, Chandel NS. ROS function in redox signaling and oxidative stress. Curr Biol 2014;24(10):R453–62.
[50] Wu H, D'Alessio AC, Ito S, Wang Z, Cui K, Zhao K, et al. Genome-wide analysis of 5-hydroxymethylcytosine distribution reveals its dual function in transcriptional regulation in mouse embryonic stem cells. Genes Dev 2011;25(7):679–84.
[51] Goldman R, Enewold L, Pellizzari E, Beach JB, Bowman ED, Krishnan SS, et al. Smoking increases carcinogenic polycyclic aromatic hydrocarbons in human lung tissue. Cancer Res 2001;61(17):6367–71.
[52] Shimada T, Fujii-Kuriyama Y. Metabolic activation of polycyclic aromatic hydrocarbons to carcinogens by cytochromes P450 1A1 and 1B1. Cancer Sci 2004;95(1):1–6.
[53] Han X, Liehr JG. Microsome-mediated 8-hydroxylation of guanine bases of DNA by steroid estrogens: correlation of DNA damage by free radicals with metabolic activation to quinones. Carcinogenesis 1995;16(10):2571–4.
[54] Parl FF, Egan KM, Li C, Crooke PS. Estrogen exposure, metabolism, and enzyme variants in a model for breast cancer risk prediction. Cancer Informat 2009;7:109–21.
[55] D'Uva G, Baci D, Albini A, Noonan DM. Cancer chemoprevention revisited: cytochrome P450 family 1B1 as a target in the tumor and the microenvironment. Cancer Treat Rev 2018;63:1–18.
[56] Gumus ZH, Du B, Kacker A, Boyle JO, Bocker JM, Mukherjee P, et al. Effects of tobacco smoke on gene expression and cellular pathways in a cellular model of oral leukoplakia. Cancer Prev Res (Phila) 2008;1(2):100–11.
[57] Steiling K, Lenburg ME, Spira A. Airway gene expression in chronic obstructive pulmonary disease. Proc Am Thorac Soc 2009;6(8):697–700.
[58] Ward JM, Nikolov NP, Tschetter JR, Kopp JB, Gonzalez FJ, Kimura S, et al. Progressive glomerulonephritis and histiocytic sarcoma associated with macrophage functional defects in CYP1B1-deficient mice. Toxicol Pathol 2004;32(6):710–8.
[59] Bird A. DNA methylation patterns and epigenetic memory. Genes Dev 2002;16(1):6–21.
[60] Yang X, Solomon S, Fraser LR, Trombino AF, Liu D, Sonenshein GE, et al. Constitutive regulation of CYP1B1 by the aryl hydrocarbon receptor (AhR) in pre-malignant and malignant mammary tissue. J Cell Biochem 2008;104(2):402–17.
[61] Lavin Y, Winter D, Blecher-Gonen R, David E, Keren-Shaul H, Merad M, et al. Tissue-resident macrophage enhancer landscapes are shaped by the local microenvironment. Cell 2014;159(6):1312–26.
[62] Xing AP, Hu XY, Shi YW, Du YC. Implication of PDGF signaling in cigarette smoke-induced pulmonary arterial hypertension in rat. Inhal Toxicol 2012;24(8):468–75.
[63] Nelson JK, Koenis DS, Scheij S, Cook EC, Moeton M, Santos A, et al. EEPD1 is a novel LXR target gene in macrophages which regulates ABCA1 abundance and cholesterol efflux. Arterioscler Thromb Vasc Biol 2017;37(3):423–32.
[64] Wu Y, Lee SH, Williamson EA, Reinert BL, Cho JH, Xia F, et al. EEPD1 rescues stressed replication forks and maintains genome stability by promoting end resection and homologous recombination repair. PLoS Genet 2015;11(12):e1005675.

Please cite this article as: M.V. Ringh, M. Hagemann-Jensen, M. Needhamsen, et al., Tobacco smoking induces changes in true DNA methylation, hydroxymethylation and gene expression in b..., EBioMedicine, https://doi.org/10.1016/j.ebiom.2019.07.006